Synthesis and Mesogenic Properties of Porphyrin Octaesters

Valerio Paganuzzi,[a] Paolo Guatteri,[a] Paola Riccardi,[a] Tania Sacchelli,[a] Joaquín Barberá,[b] Mirco Costa,*[a] and Enrico Dalcanale*[a]

Keywords: 3,4-Disubstituted pyrroles / Porphyrin octaesters / Liquid crystals / π-π interactions

A new and efficient method of preparing 3,4-pyrrolediacetic esters **3** is reported, together with their conversion, according to the Lindsey procedure, to a series of octa- and dodecasubstituted porphyrins. This procedure, which consists of a palladium-catalysed oxidative alkoxycarbonylation of *N*-substituted dipropargylamine derivatives **1**, works nicely for *n*-alkyl alcohols in the range C_1 to C_{14}. The thermotropic behaviour of this series of porphyrins (28 compounds) has been investigated using polarization microscopy, DSC, X-ray diffraction, and miscibility tests. The planarity of the macrocyclic core constitutes the major structural requirement for mesophase formation. The mesophase temperature range is controlled by the length of the side chains through the melting point and by the strength of π-π interactions among the cores through the clearing point. The same set of rules governing porphyrin packing in the solid state can be employed to predict mesophase formation and organization in porphyrin octaesters

Introduction

Attempts to find applications for porphyrins and related compounds as the framework of new materials have increased significantly in the last few years.[1] In particular, liquid-crystalline porphyrins have received considerable attention as materials for molecular electronics, due to their peculiar properties as unidimensional conductors[2] and semiconductors.[3]

Mesogenic columnar porphyrins[4] present several features ideal to this purpose: the ability to self-organize in well-ordered, fluid structures; the organized stacking of the macrocyclic cores with extensive π-electronic systems at interacting distances; the presence of a large number of aliphatic tails which act as insulators among columns, and the possibility to insert metal ions to alter the redox properties of the molecules. Furthermore, the self-organization potential of the liquid-crystalline phase allows the deposition of extremely ordered Langmuir−Blodgett films formed by columnar stacks of porphyrins parallel to the support.[5]

Mesogenic porphyrins can be divided into two broad categories depending upon the location of the substituents about the macrocyclic ring and the number of side chains:[6]

− Porphyrins, octasubstituted at the β-positions of the pyrrole rings (structure **I**)

− Porphyrins di- and tetrasubstituted at the *meso* positions (structure **II**)

All the liquid-crystalline β-octasubstituted porphyrins exhibit columnar mesophases, while *meso*-aryl-substituted porphyrins form discotic lamellar phases (D_L),[7] nematic/smectic phases,[8] and hexagonal columnar phases,[9] depending on the number and nature of substituents.

Until now, mesogenic β-octasubstituted porphyrins have been prepared following a laborious synthetic procedure[10] which requires the preparation of tetrafunctionalized pyrroles as precursors.[11]

The present limited availability of 3,4-disubstituted pyrroles, which are the basic precursors in some synthetic procedures, constitutes the largest drawback in the synthesis of octasubstituted porphyrins.[12] Some years ago Lindsey et al. reported a new method for the synthesis of porphyrins under extremely mild conditions.[13] According to this method, pyrroles and aliphatic or preferentially aromatic aldehydes are allowed to react in sequential condensation and oxidation steps at room temperature in the presence of trifluoroacetic acid or $BF_3 \cdot Et_2O$. The gentle conditions enable aldehydes that are functionalized with sensitive groups to be converted directly to the corresponding porphyrins.

Here we report the synthesis of porphyrin octaesters, based on a new and efficient method of preparation of 3,4-pyrrolediacetic esters and their direct condensation with paraformaldehyde and aromatic aldehydes using the Lindsey protocol. This new procedure allows easy access to a whole set of octa- and dodecasubstituted porphyrins and their metal complexes, allowing for the in-depth study of the structural requirements for mesophase formation and stability in this class of porphyrins. π-π interactions have been identified as the driving force for aggregation of metalated porphyrins, both in the solid state and in solution.[14] However, this issue has been addressed only in one case for mesogenic porphyrins, without reaching any clear conclusion.[10b] In this paper we demonstrate, for the first time, that π-π interactions dictate the mesophase organization, and that they

[a] Dipartimento di Chimica Organica e Industriale, Università di Parma,
Parco Area delle Scienze 17/A, I-43100 Parma, Italy
Fax: (internat.) + 39-0521/905472
E-mail: costa@ipruniv.cce.unipr.it
dalcanal@ipruniv.cce.unipr.it
[b] Química Orgánica, Facultad de Ciencias ICMA, Univesidad de Zaragoza, CSIC
E-50009 Zaragoza, Spain

  1434−193X/99/0707−1527 $ 17.50+.50/0

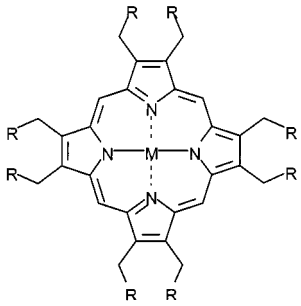

I

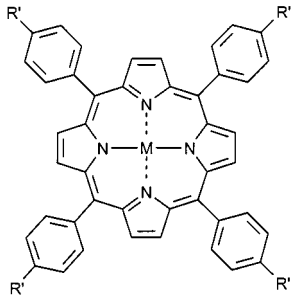

II

M = 2 H, metal; R = $COOC_nH_{2n+1}$, n = 4, 6, 8; R = $CH_2OC_nH_{2n+1}$, n = 4, 6, 8, 10; R′ = C_nH_{2n+1}, n = 5−16; R′ = OC_nH_{2n+1}, n = 5−14, 18; R′ = $COOC_nH_{2n+1}$, n = 12, 16, 18

contribute, when the planarity of the porphyrin core is maintained, to the enhancement of the thermal stability of the mesophase, by increasing the clearing point.

Results and Discussion

Synthesis of Long-Chain Pyrrole-3,4-diacetic Esters

Our procedure for the synthesis of pyrrole-3,4-diacetic esters consists of the palladium-catalyzed oxidative alkoxycarbonylation, with simultaneous cyclization, of the readily accessible dipropargylamine (**1**) and its *N*-substituted derivatives, followed by an isomerization step as shown in Scheme 1.[15]

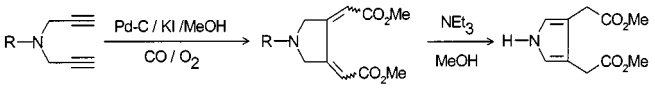

1 **2** **3a**

Scheme 1. Synthetic route to pyrrole diester **3a**: R = formyl, acetyl, benzoyl, alkoxycarbonyl

Both steps proceed under mild conditions. The oxidative alkoxycarbonylation step leads to a mixture of stereomeric 3,4-bis(methoxycarbonylmethylene)pyrrolidines **2**, which are converted into **3a** upon treatment with triethylamine in methanol.

Having in hand this promising procedure, we considered the possibility of extending it to the direct preparation of long-chain pyrrole diesters **3b**−**h** (Scheme 2). DMA was introduced as a cosolvent with the dual purpose of solubilizing the palladium ion as K_2PdI_4 in the reaction medium (since it is insoluble in long-chain aliphatic alcohols) and of promoting the isomerization of pyrrolidines to pyrroles. Carbonylation reactions were carried out in an autoclave under a total pressure of 22 bar (16 bar of CO and 6 bar of air) at 60°C for 72 h, using a 6:4 mixture of alcohol/DMA. 10% palladium on activated carbon was used as the catalyst, and KI as a promoter.

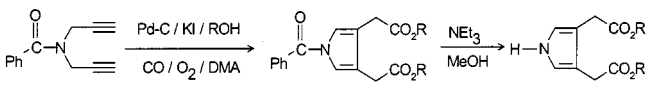

4b-h **3b-h**

Scheme 2. Synthetic route to long-chain pyrrole diesters **3b**−**h**

The reaction works well for a wide spectrum of *n*-alkyl derivatives in the range C_3 to C_{14}. In all cases the sole carbonylation product was the pyrrole diester **4**, obtained in 33−45% yield depending on the alcohol used (Table 1). About 5% of the starting amide was recovered at the end of the carbonylation reaction. The remainder of the reaction mixture consisted of highly carbonylated products, which were not characterised. No trace of the pyrrolidine isomers **2**, usually formed in this type of carbonylation, was detected under these conditions. The double bond shift inside the ring can be attributed to the basicity of DMA.

Removal of the benzoyl group to give the desired pyrrole **3** is easily achieved in NEt_3/CH_3OH at room temperature in 60−75% isolated yields, without formation of transesterification byproducts.

Table 1. Yields of carbonylation and deprotection steps in the pyrrole-3,4-diacetic esters synthesis

ROH R =	Yield (%)[a] **4**	Yield (%)[b] **3**
C_3H_7 (**b**)	42	75
C_6H_{13} (**c**)	45	60
C_8H_{17} (**d**)	41	74
$C_{10}H_{21}$ (**e**)	43	75
$C_{11}H_{23}$ (**f**)	42	66
$C_{12}H_{25}$ (**g**)	38	75
$C_{14}H_{29}$ (**h**)	33	75

[a] Yields of isolated products referred to the starting acetylenic derivative. − [b] Yields of isolated products referred to the starting **4b**−**h**.

Synthesis of Octa- and Dodecasubstituted Porphyrins: Octaalkyl Porphyrin-2,3,7,8,12,13,17,18-octacetates and Their Metal Complexes

The synthesis of octaalkyl porphyrinoctaacetates (**H_2C_nOAP**) was carried out by condensing paraformaldehyde with the corresponding pyrrole-3,4-diacetic ester **3b**−**h** in the presence of $BF_3 \cdot Et_2O$ as catalyst, using a modification of the procedure reported by Lindsey et al. for **H_2TPP** and aliphatic *meso*-substituted porphyrins (Scheme 3).[13]

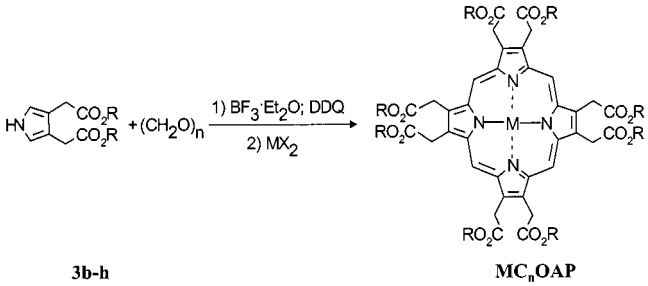

3b-h **MC_nOAP**

Scheme 3. Preparation of porphyrin octaesters H_2C***n***OAP and their metal derivatives MC***n***OAP: R = C_nH_{2n+1}, n = 3, 6, 8, 10, 11, 12, 14; M = 2 H, Zn; R = $C_{10}H_{21}$; M = Cd, Cu, Ni, Pb, Pd, Pt, Zn

Longer times either in the condensation step (3−4 h) or in the oxidation step with DDQ (16 h) were required. A

concentration of the reagents (equimolar with respect to paraformaldehyde and **3b**−**h**) of $5 \cdot 10^{-3}$ M was used. This is an intermediate value with respect to the values of $1 \cdot 10^{-2}$ M and $1 \cdot 10^{-3}$ M, usually used for **H_2TPP** and the *meso*-alkylporphyrins, respectively. Finally, before adding DDQ, the acid was

neutralized with triethylamine (1 mol-equiv. relative to BF_3). Purification of the crude products by column chromatography on Florisil, followed by recrystallization from dichloromethane/methanol afforded the pure porphyrins in relatively high yields (31−48%).

The corresponding Zn complexes (**ZnC$_n$OAP**) were prepared according to methods reported in the literature.[16] Other metalated porphyrins **MC$_{10}$OAP** (M = Cd, Cu, Ni, Pb[17], Pd, Pt[18]) were also prepared.

Octaalkyl 5,10,15,20-Tetraarylporphyrin-2,3,7,8,12,13,17,18-octaacetates and Their Metal Complexes

Extension of the modified Lindsey procedure reported above, to the synthesis of tetraarylporphyrin octaesters (**H_2OATPP**) using benzaldehyde and *para*-alkoxy-substituted benzaldehydes led to the formation of the desired compounds, albeit in low yields.

The condensation of **3d** with benzaldehyde and *p*-octyloxybenzaldehyde afforded porphyrins **H_2C_8OATPP** and **$H_2C_8OAC_8$TPP** in 26% and 15% yield, respectively (Scheme 4). Under the same conditions, reaction of **3g** with *p*-dodecyloxybenzaldehyde gave **$H_2C_{12}OAC_{12}$TPP** in 23% isolated yield. The low yields obtained in the preparation of dodeca-substituted porphyrins are due to their inherent instability, caused by the non-planarity of the porphyrin core. As a result, these compounds must be stored under argon. Metalation with Zn or Cu improves the stability of the corresponding metal complexes in air. All dodeca-substituted porphyrins and their metal complexes are isotropic liquids, which do not crystallize even if kept for long time at 250 K. DSC measurements performed on the metal complexes, which are stable, showed the absence of any transition down to 238 K.

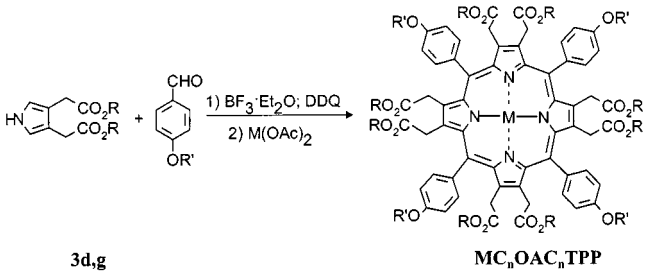

Scheme 4. Preparation of dodecasubstituted porphyrins H_2C*n*OAC*n*TPP and their metal derivatives MC*n*OAC*n*TPP: R = R′ = C_nH_{2n+1}, n = 8, 12; M = 2 H, Zn; R = R′ = C_nH_{2n+1}, n = 8; M = Cu

Core Conformation

It is a well-known fact that deviations from planarity in the porphyrin core depend critically on the number and nat-

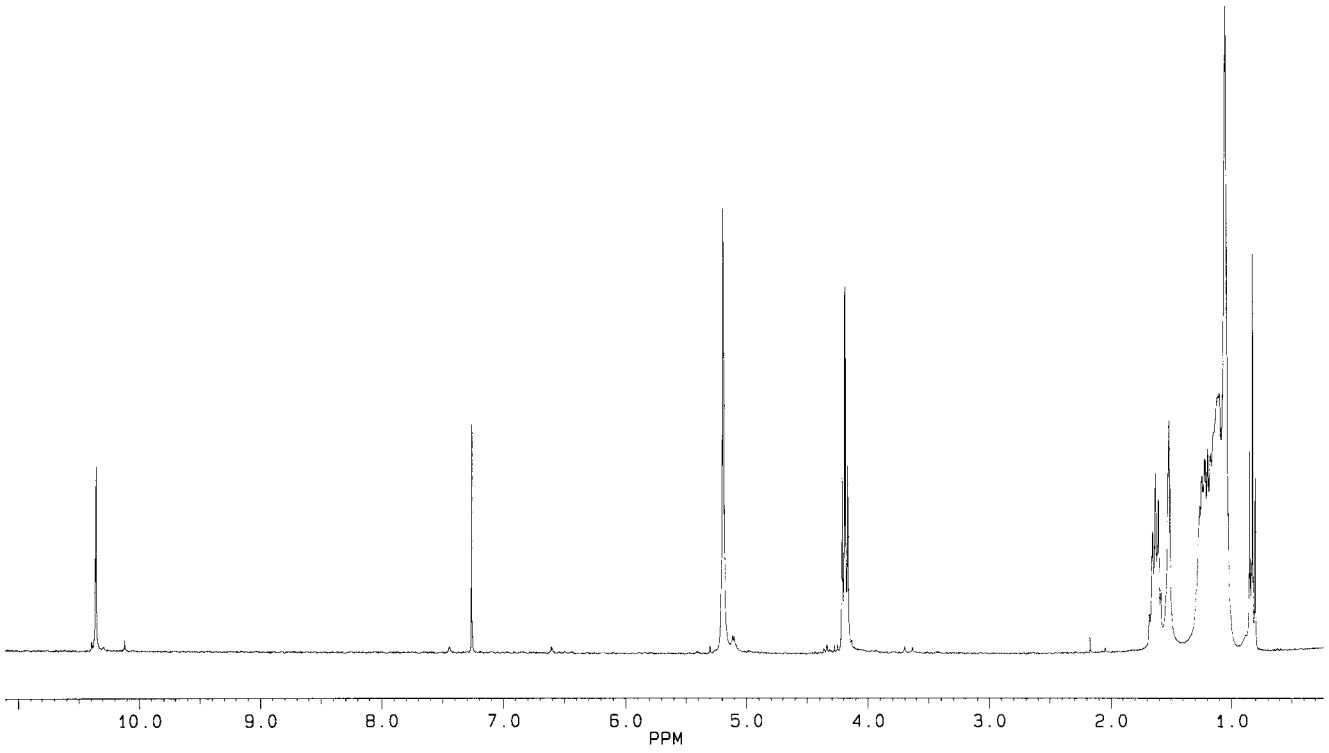

Figure 1. ^{1}H-NMR spectrum of **ZnC$_{10}$OAP** in $CDCl_3$ at 300 K

ure of peripheral substituents.[19] In particular, dodeca-substituted porphyrins assume a significantly distorted saddle conformation both in the solid state and in solution in order to minimize steric crowding among *meso* and β substituents.[20] Removal of the four *meso* substituents restores planarity in β-octasubstituted porphyrins, and in their metal complexes, provided that the metal ion can be fully accomodated into the macrocycle hole.

The simplest way to evaluate conformational distortion in our long-chain-substituted porphyrins, unsuitable for single-crystal X-ray analysis, is variable-temperature ^{1}H NMR. The splitting of the singlet α-CH_2 resonance (the methylene groups connecting the pyrrole rings to the ester chains) into diastereotopic doublets is diagnostic of the non-equivalence of the two sides of the macrocycle, generated by conformational distortion.

All β-octasubstituted porphyrins **H_2C_nOAP** and their metal complexes **MC_nOAP** are planar (Figure 1). The only exception is **$PbC_{10}OAP$**, whose ^{1}H-NMR spectrum at 300 K shows a pair of doublets for the α-CH_2 protons at $\delta = 5.11$ and $\delta = 5.19$. By heating to 330 K in $CDCl_3$ this pattern does not change. This inequivalence of the α-CH_2 protons is due to the out-of-plane position of the Pb^{II} ion due to its large size, which forces the macrocycle to assume a dome-shaped conformation.[21]

All dodeca-substituted porphyrins, with the exception of **ZnC_8OATPP**, exhibit diastereotopic α-CH_2 protons at room temperature, which indicate that they adopt a non-planar saddle conformation in solution. In the case of the free-base derivatives **$H_2C_nOAC_nTPP$** (n = 8 or 12) no significant methylene signal broadening is observed upon warming to 383 K, while for their zinc complexes **ZnC_8OAC_8TPP** and **$ZnC_{12}OAC_{12}TPP$** coalescence of the two broad singlets takes place at 330 K. **ZnC_8OATPP** in contrast, is fluxional, showing a broad singlet for its α-CH_2 protons already at 300 K. By cooling to 270 K the broad singlet is split into two sharp doublets. Therefore, as expected,[22] complexation with zinc ion significantly reduces the activation energy for the ring inversion process in these porphyrins.

Another well-known indicator of non-planar distortion in porphyrins is the red-shift of the Soret band.[23] The absorption maxima of all dodeca-substituted porphyrins prepared are red-shifted compared to the β-octasubstituted ones (see Experimental Section). The red-shift is also present in **$PbC_{10}OAP$** and, to a lesser extent, in **$CdC_{10}OAP$**, supporting the presence of a small out-of-plane displacement of Cd^{II} not evidenced by ^{1}H NMR.[24]

Mesogenic Properties

The mesogenic properties of β-octasubstituted porphyrins were investigated using optical microscopy (OM), differential scanning calorimetry (DSC), X-ray diffraction, and miscibility studies. Their thermal behaviour and phase organization deduced from these techniques are summarized in Tables 2 and 3, and graphically shown in the phase diagrams of Figures 2 and 3. All the OM observations are consistent with the DSC traces. All porphyrin octaesters are solids at room temperature, while all dodeca-substituted derivatives are isotropic liquids. All transitions are reversible, although some supercooling is observed for liquid-to-mesophase and mesophase-to-solid transitions.

Preparation of porphyrin octaesters and their zinc complexes having side-chain extension from C_3 to C_{14} have allowed us to define the mesophase stability range with respect to the number of carbon atoms in the eight alkoxycarbonyl side chains. **H_2C_3OAP** and **ZnC_3OAP** are not mesogenic, with the former presenting a crystal-to-crystal phase transition, both in the heating and cooling cycles. Comparison of the behavior of **ZnC_3OAP** with that of **ZnC_4OAP** from the literature[10a] allows us to establish that a minimum of four carbon atoms is necessary in the side chains for mesophase injection in porphyrin octaesters.

Porphyrins **H_2C_6OAP**, **ZnC_6OAP**, **H_2C_8OAP**, and **ZnC_8OAP** have been described previously by Gregg et al.[10a] Our DSC traces confirm the presence of two enantiotropic phases having slightly different transition temperatures with respect to the reported ones, mostly due to the different heating rates used. For all of them the clearing enthalpies are larger or comparable to the melting enthalpies, indicating the formation of highly ordered phases. Our OM observations, however, attribute the first transition to a crystal-to-crystal transition and not to the formation of a highly viscous mesophase. Since this transition is present only in C_6 and C_8 derivatives, it has not been investigated further. **$H_2C_{10}OAP$**, **$H_2C_{11}OAP$**, **$H_2C_{12}OAP$**, **$H_2C_{14}OAP$**, and their Zn complexes exhibit an enantiotropic mesophase with clearing enthalpies smaller than their melting enthalpies.

The mesophase temperature range shows a significant decrease for **$H_2C_{14}OAP$** and **$ZnC_{14}OAP$** with respect to the previous homologues. This trend has not been investigated further due to synthetic difficulties in the preparation of longer chain pyrrole diacetic esters.

$H_2C_{10}OAP$ and **$ZnC_{10}OAP$** were examined at their room-temperature and high-temperature phases by powder X-ray diffraction, using a Pinhole camera equipped with a variable-temperature sample holder. For the two compounds, the X-ray photographs taken at room temperature indicate the 3D-crystalline nature of the virgin powder as well as of the solid recrystallized from the mesophase. This is revealed by the presence of numerous sharp rings over the whole angular range of the patterns. This is consistent with the OM and DSC observations. On the other hand, the high-temperature photographs are characteristic of a liquid-crystal phase: they contain a set of sharp rings at small angles, but in the large-angle region no diffraction rings are detected, and a diffuse halo is observed instead. The registered reflections are consistent with an orthorhombic lattice. Table 4 collects the experimentally measured and calculated spacing, the proposed indexing, and the lattice constants. The absence of reflections with Miller index l different from zero reveals the two-dimensional character of the structure, and at the same time indicates that there is no

Table 2. Transition temperatures [°C][a] and enthalpies ΔH [kJmol^{-1}] for **H_2C_nOAP** and **ZnC_nOAP**

Compound	Transition[b]	T [°C]	ΔH [kJmol^{-1}]	Transition[c]	T [°C]	ΔH [kJmol^{-1}]
H_2C_3OAP	$I-K'$	241	44.9	$K-K'$	163	5.3
	$K'-K$	149	5.8	$K'-I$	249	44.2
ZnC_3OAP	$I-K$	283	26.6	$K-I$	297	26.8
H_2C_6OAP	$I-D_r$	177	43.8	$K-K'$	66	18.0
	D_r-K'	122	23.4	$K'-D_r$	135	22.7
	$K'-K$	38	18.5	D_r-I	191	44.2
ZnC_6OAP	$I-D_r$	218	29.1	$K-K'$	60	20.5
	D_r-K'	124	15.6	$K'-D_r$	135	15.4
	$K'-K$	28	16.9	D_r-I	230	27.8
H_2C_8OAP	$I-D_r$	160	24.5	$K-K'$	102	25.1
	D_r-K'	104	29.3	$K'-D_r$	112	28.8
	$K'-K$	86	28.8	D_r-I	171	29.0
ZnC_8OAP	$I-D_r$	201	26.1	$K-K'$	98	26.2
	D_r-K'	105	26.9	$K'-D_r$	113	26.1
	$K'-K$	84	30.0	D_r-I	211	26.6
$H_2C_{10}OAP$	$I-D_r$	149	21.6	$K-D_r$	110	79.6
	D_r-K	90	90.4	D_r-I	159	18.1
$ZnC_{10}OAP$	$I-D_r$	183	16.9	$K-D_r$	110	68.6
	D_r-K	91	74.8	D_r-I	194	17.0
$H_2C_{11}OAP$	$I-D_r$	149	17.4	$K-D_r$	106	54.5
	D_r-K	83	60.7	D_r-I	166	16.7
$ZnC_{11}OAP$	$I-D_r$	167	5.7	$K-D_r$	99	30.5
	D_r-K	79	30.9	D_r-I	186	4.2
$H_2C_{12}OAP$	$I-D_r$	151	16.2	$K-D_r$	116	71.4
	D_r-K	90	60.1	D_r-I	160	16.8
$ZnC_{12}OAP$	$I-D_r$	182	26.3	$K-D_r$	113	100.3
	D_r-K	91	99.7	D_r-I	189	26.7
$H_2C_{14}OAP$	$I-D_r$	131	6.2	$K-D_r$	117	75.2
	D_r-K	93	53.7	D_r-I	140	5.2
$ZnC_{14}OAP$	$I-D_r$	167	6.9	$K-D_r$	114	43.5
	D_r-K	87	50.8	D_r-I	180	5.3

[a] Taken from the maximum of the peaks. – [b] Cooling run 20°C/min. – [c] Second heating run 20°C/min.

order inside the columns, i.e. there is no fixed stacking distance. For all the reflections observed in both compounds $h + k = 2n$, which indicates that the lattice is centered on the AB plane, i.e. it is a C-centered orthorhombic lattice. All these features are consistent with a rectangular columnar mesophase with a space group $C2/m$.[25] In this mesophase, the disc-like molecules stack one on top of another and the columns generated adopt a rectangular packing with the column axes located at the corners and at the center of the rectangle. The structure of the mesophase is the same for both compounds, with a slight difference in the lattice parameters. It is interesting to note that for the zinc-containing complex a higher number of reflections are observed than for the free porphyrin. This is expected as the presence of the metal atom increases the structure factor at wide angles, and reinforces the intensity of diffraction peaks over the whole angular range.[26] The halo centered at 4.6 Å is usually found in discotic mesophases, and it is associated with the short-range inter-disc correlation and with the liquid-like correlation between the conformationally disordered hydrocarbon chains.[25]

All metal complexes, with the exception of **$PbC_{10}OAP$**, form a single enantiotropic column mesophase, indexed as D_r by miscibility studies with **$ZnC_{10}OAP$**.

Distortion from planarity strongly disfavors π stacking among porphyrins and therefore columnar organization. This is shown by all dodeca-substituted porphyrins synthesized, none of which is mesogenic, despite of the presence of twelve long alkyl chains radiating from the core. Introduction of a metal ion does not suffice to impart liquid crystallinity to them. Even the out-of-plane displacement of Pb^{II} in **$PbC_{10}OAP$** is sufficient to suppress mesophase formation.[27][28] Therefore, the major structural requirement necessary to impart liquid-crystalline properties to porphyrin octaesters is the absence of significant deviations from planarity of the macrocyclic core. Distortion from planarity also has the effect of depressing the melting point of these compounds (Table 3).

Table 3. Transition temperatures [°C][a] and enthalpies ΔH [kJmol^{-1}] for **MC$_{10}$OAP**

Compound	Transition[b]	T [°C]	ΔH [kJmol^{-1}]	Transition[c]	T [°C]	ΔH [kJmol^{-1}]
PtC$_{10}$OAP	$I-D_r$	198	17.3	$K-D_r$	111	46.7
	D_r-K	93	49.5	D_r-I	210	17.8
PdC$_{10}$OAP	$I-D_r$	189	20.6	$K-D_r$	101	60.9
	D_r-K	86	64.3	D_r-I	203	21.2
ZnC$_{10}$OAP	$I-D_r$	183	16.9	$K-D_r$	110	68.6
	D_r-K	91	74.8	D_r-I	194	17.0
CuC$_{10}$OAP	$I-D_r$	177	10.8	$K-D_r$	101	38.5
	D_r-K	85	37.7	D_r-I	191	10.6
CdC$_{10}$OAP	$I-D_r$	164	11.2	$K-D_r$	111	57.6
	D_r-K	89	64.4	D_r-I	177	10.0
NiC$_{10}$OAP	$I-D_r$	156	15.8	$K-D_r$	104	69.4
	D_r-K	83	67.1	D_r-I	168	16.9
PbC$_{10}$OAP	$I-K$	47	34.2	$K-I$	69	32.8

[a] Taken from the maximum of the peaks. – [b] Cooling run 20°C/min. – [c] Second heating run 20°C/min.

Table 4. X-ray diffraction data for the mesophase of porphyrins **H$_2$C$_{10}$OAP** and **ZnC$_{10}$OAP**

Compound	Temperature [°C]	$h\ k\ l$	$d_{obsd.}$ [Å]	$d_{calcd.}$ [Å]	Lattice constants [Å]
H$_2$C$_{10}$OAP	120	2 0 0	26.87	26.95	a = 53.9
		1 1 0	23.48	23.49	b = 26.1
		3 1 0	14.82	14.80	
		4 0 0	13.51	13.47	
				4.6 (br.)	
ZnC$_{10}$OAP	120	2 0 0	27.44	27.40	a = 54.8
		1 1 0	24.11	24.08	b = 26.8
		3 1 0	15.14	15.09	
		4 0 0	13.60	13.70	
		2 2 0	12.00	12.04	
		5 1 0	10.20	10.14	
		4 4 0	5.98	6.02	
				4.6 (br.)	

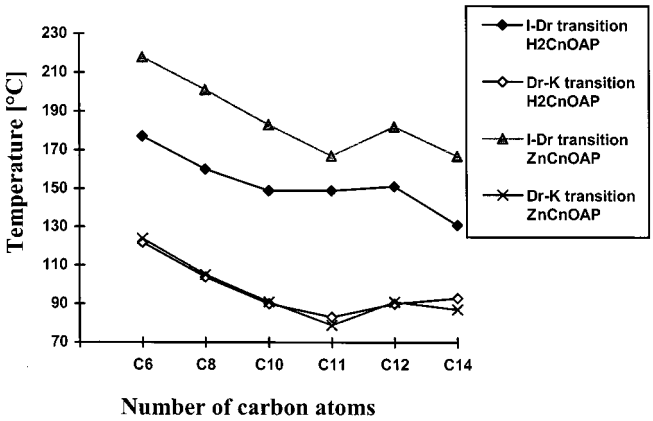

Figure 2. Phase diagram for **H$_2$C$_n$OAP** and **ZnC$_n$OAP** based on DSC measurements (cooling cycle)

The Role of π-π Interactions in the Mesophase Self-Organization of Porphyrin Octaesters

As is clearly shown in Figure 2, the incorporation of Zn into the porphyrins stabilizes the columnar mesophase by increasing the clearing-point temperature, with almost no effect on the crystal-to-mesophase transition. This behavior is consistent with the accepted mechanism for mesophase formation in discotic liquid crystals, which predicts that the melting temperatures are controlled by the side-chain structure, while the clearing temperatures (i.e. the unstacking of the cores) depend mainly on the strength of the interactions among the cores.[29]

The general tendency of metal complexation to enhance porphyrin self-aggregation, both in the solid state and in solution, has been rationalized in terms of favorable electrostatic interactions between the metal ion placed in the cavity of the porphyrin ring and the π-electrons of the pyrrole of another porphyrin.[14] The extension of this rationalization to the prediction of mesophase stability, where the columnar self-organization is the result of many cooperative steric and electrostatic interactions among stacked porphyrins, is not straightforward.

In order to understand the origin of this stabilization we prepared different metal complexes of the C_{10} porphyrin **MC$_{10}$OAP**, and compared their mesogenic properties (Table 3).

Figure 3 shows that the mesophase-to-crystal transition temperature is similar for all **MC$_{10}$OAP** complexes, as expected. The isotropic liquid-to-mesophase transition temperature, however. is highly influenced by the complexed metal ion. The relative strength of core-to-core interactions, expressed by the isotropic liquid-to-mesophase transition temperature is: **PtC$_{10}$OAP** (198 °C) > **PdC$_{10}$OAP** (189 °C) > **ZnC$_{10}$OAP** (183 °C) > **CuC$_{10}$OAP** (177 °C) > **CdC$_{10}$OAP** (164 °C) > **NiC$_{10}$OAP** (156 °C) > **H$_2$C$_{10}$OAP** (149 °C). The same trend is observed for the clearing points (see Table 3): **PtC$_{10}$OAP** (210 °C) > **PdC$_{10}$OAP** (203 °C) > **ZnC$_{10}$OAP** (194 °C) > **CuC$_{10}$OAP** (191 °C) > **CdC$_{10}$OAP** (177 °C) > **NiC$_{10}$OAP** (168 °C) > **H$_2$C$_{10}$OAP** (159 °C).

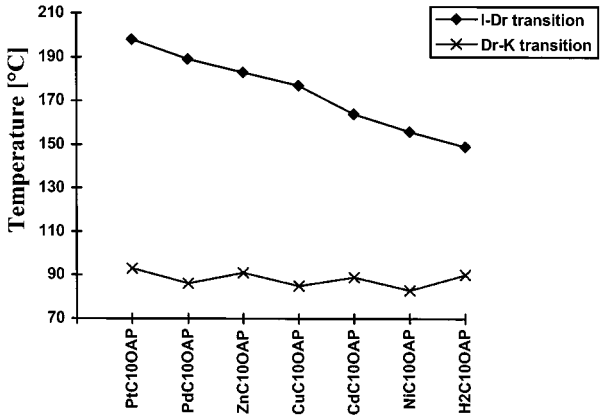

Figure 3. Phase diagram for **$MC_{10}OAP$** based on DSC measurements (cooling cycle)

In the solid state, planar porphyrins form extended one-dimensional aggregates with the molecules arranged parallel to each other in a slipped geometry optimal for π-π interactions.[30] This aggregation mode is retained in the mesophase, which is discotic biaxial (D_r), where the molecules stack in columns in the offset mode. The alternative uniaxial (D_h) mesophase organization, which requires aligned packing of the molecules, is not observed (Figure 4). Moreover, in the mesophase as in the solid state, metalation has no effect on the geometry of π-π interaction, but only on its magnitude.

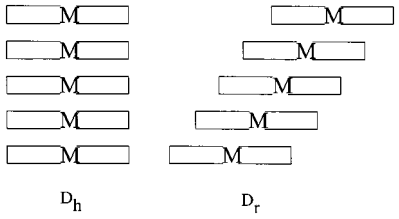

Figure 4. The two general types of packing modes found in columnar mesophases: hexagonal D_h (uniaxial) and rectangular D_r (biaxial); porphyrin octaesters form exclusively D_r mesophases (space group *C*2/*m*)

Since the mesophase organization of porphyrin octaesters nicely reproduces the offset mode indicated by the model of Hunter and Sanders, we further tested the predictive value of the model by correlating the observed trend in the clearing points/isotropic liquid-to-mesophase transitions of **$MC_{10}OAP$** to a suitable physico-chemical parameter.

First we attempted to relate the clearing points with the effective ionic radii of the divalent ions in the square-planar coordination.[31] The overall trend of Figure 3 cannot be reproduced on the basis of this single parameter. However, this correlation points out an effective ionic radius of ca. 0.6 Å as the optimal value for mesophase stabilization (see Cu, Pt, Zn, and Pd values of Table 5). The relative depression of the clearing points produced by the larger ions Cd^{II} and Pb^{II} can be rationalized in terms of size-induced non-planarity of the porphyrin core. According to the model, pulling the metal ion out of the plane of the porphyrin results in a reduction of the strength of σ-π interaction, which in the case of **$CdC_{10}OAP$**, should correspond to a depression of the clearing point. Non-planar distortions are also produced in octasubstituted porphyrins by complexation with small ions like Ni^{II}, as reported in the literature,[32] because the distortion allows the porphyrin core to contract around the metal ion. The presence of metal-induced non-planar conformations should make the π-π stacking in **$NiC_{10}OAP$** less efficient, therefore depressing the clearing points.

A parameter which could account for the effective positive charge which resides on the metal ion is the electronegativity scale of Allred−Rochow,[33] in which both the effective nuclear charge and the dimensions of the ions are considered. The lower the electronegative character of the ion, the stronger should be the σ-π electrostatic attractive interaction among porphyrins. According to this scale, the predicted order of mesophase stability is: **$PdC_{10}OAP$** > **$PtC_{10}OAP$** > **$CdC_{10}OAP$** > **$ZnC_{10}OAP$** > **$CuC_{10}OAP$** ≈ **$NiC_{10}OAP$** (Table 5). This parameter is better than the previous one at reproducing the experimental trend, but still not sufficiently well. However, if the destabilizing non-planar conformational distortions present in **$CdC_{10}OAP$** and, to a lesser extent, in **$NiC_{10}OAP$** are taken into account, the overall trend can be qualitatively understood. Nevertheless, the predictive value of these correlations is still low if applied to other mesogenic octasubstituted porphyrins,[10b,34] suggesting that also the nature of the β-substituents plays a role.

A correlation between the oxidation potentials of the porphyrins and the extent of π-π aggregation in solution has been demonstrated.[35] Our attempts to correlate the oxidation potentials of **$MC_{10}OAP$**[36] with the trend shown in Figure 3 gave no appreciable results, anologously to the results reported by Gregg et al. on a different class of liquid-crystalline porphyrins.[10b]

Table 5. Effective ionic radii [Å] and Allred−Rochow electronegativity values of selected divalent metal ions M^{II}

Ion	Ni^{II}	Cu^{II}	Zn^{II}
Ionic radius	0.49	0.57	0.60
Allred−Rochow value	1.75	1.75	1.66
Ion	Pd^{II}		Cd^{II}
Ionic radius	0.64		0.78
Allred−Rochow value	1.35		1.46
Ion	Pt^{II}		Pb^{II}
Ionic radius	0.60		0.98
Allred−Rochow value	1.44		1.55

Conclusions

We have developed a new catalytic procedure for the synthesis of 3,4-pyrrolediacetic esters starting from the readily accessible *N*,*N*-dipropargylbenzamide, which has allowed us to prepare 28 different porphyrins, and to study their mesogenic properties in detail.

The thermotropic behaviour of these compounds has been investigated as function of (i) conformation of the

macrocyclic core, (ii) length of the side chains, and (iii) size and type of the complexed metal ion.

All planar porphyrin octaesters with side chains residues longer than C_3 form D_r columnar mesophases. Significant deviation from planarity of the macrocyclic core, caused either by the presence of *meso* substituents or by complexation of metal ions larger than the cavity size (like Pb^{II}) completely suppress mesophase formation.

The collected data indicate that the formation of columnar mesophases in porphyrin octaesters is a typical phenomenon of self-organization, induced by the shape of the constituent molecules and by specific interactions among them. D_r mesophase organization is dictated by π-π interactions, which require an offset geometry to stabilize the stacking of the porphyrin cores in the columns. The mesophase temperature range is a function of two distinct structural parameters: the length of the side chains − which controls the melting temperatures; and the type and size of the complexed metal − which affects the clearing temperatures by tuning the strength of π-π interactions. The influence of the complexed metal ion on π-π interactions is both electrostatic and geometric in nature. Metalation places a positive charge in the porphyrin core, which has the general effect of widening the mesophase temperature range by raising the clearing point. Non-planar conformational distortions of the porphyrin core, caused by metal ions too large to fit exactly in the central cavity of the macrocycle, are destabilizing for π-π interactions. The balance between these two factors determines the relative stability of the columnar mesophase in **MC$_n$OAP**s.

Experimental Section

General: ACS-grade reagents were used without further purification. Ethyl ether was distilled under nitrogen from sodium ketyl, while the other solvents were dried with 3-Å molecular sieves. − Analytical TLC was performed on Merck silica gel or aluminum oxide 60 F_{254} precoated plates. − Preparative TLC employed glass-backed silica gel or aluminum oxide plates (Merck, 60 F_{254}). − Column chromatography was performed using silica gel or aluminum oxide (Merck, 70−230 mesh ASTM) or florisil activated at 80°C for 3 h. − Analyses of the volatile products were carried out by GLC. − ^{1}H-NMR spectra were recorded at 400, 300, and 100 MHz. Chemical shifts are given in ppm ($\delta_{TMS} = 0$) using the residual resonances of the deuterated solvents (δ = 7.25 for chloroform; δ = 6.00 for 1,1,2,2-tetrachloroethane) as internal references. − IR spectra were recorded with an FT-IR spectrometer. − Mass spectra were recorded with a single-stage quadrupole mass spectrometer using the CI technique. − UV/Vis spectra were recorded with a spectrophotometer. − Melting points were found using an electrothermal melting-point apparatus, and are uncorrected. − Optical microscopy was performed using a Leitz−Wetzlar polarizing microscope, equipped with a Mettler FP 82 hot stage. Samples were observed as a thin layer between two glass cover slips. − DSC measurements were made with a Perkin−Elmer DSC 7 thermal analyzer. The apparatus was calibrated with indium (156.6°C; 28.4 J/g). Reproducible traces were obtained for all compounds during the second and subsequent heating-cooling cycles (scanning rate 20 °Cmin^{-1}). − X-ray diffraction experiments were carried out on powder samples in a Pinhole camera (Anton−Paar) operating with a Ni-filtered Cu-K_α beam. The samples were held in Lindemann glass capillaries (1 mm diameter) and heated with a variable-temperature attachment. The X-ray patterns were collected on flat photographic film. − *N*,*N*-Dipropargylbenzamide was prepared according to a published procedure.[15]

General Procedure for the Synthesis of the Dialkyl *N*-Benzoylpyrrole-3,4-diacetates 4b−4h: In a 500-mL stainless steel autoclave, air-filled at atmospheric pressure, were placed *N*,*N*-dipropargylbenzamide (7.61 mmol), 10% Pd on carbon (0.38 mmol), KI (7.61 mmol), and a mixture alcohol/DMA (6:4). The autoclave was pressurized with 20 bar CO and air up to 25 bar, and the contents were kept at 60°C for 72 h with stirring. The reaction mixture of the carbonylated products was filtered and the filtered solution was washed with water. Distillation at reduced pressure removed the DMA and excess alcohol.

Dipropyl *N*-Benzoylpyrrole-3,4-diacetate (4b): The crude product was purified by silica gel column chromatography with hexane/ethyl acetate (8:2) as eluant to give **4b** (yellow oil) in 42% yield. − ^{1}H NMR (300 MHz, $CDCl_3$): δ = 0.92 (t, *J* = 7.4 Hz, 6 H, CH_3), 1.63 (m, 4 H, CH_2CH_3), 3.49 (s, 4 H, CH_2COO), 4.05 (t, *J* = 6.7 Hz, 4 H, $COOCH_2$), 7.21 (s, 2 H, H^α), 7.45 (m, 2 H, H^m), 7.55 (m, 1 H, H^p), 7.72 (m, 2 H, H^o). − FT IR (film): $\tilde{\nu}$ = 1737 cm^{-1} (C=O ester), 1696 (C=O amide), 1178 (C−O). − MS (CI); *m*/*z* (%): 371 (100) [M$^+$].

Dihexyl *N*-Benzoylpyrrole-3,4-diacetate (4c): The crude product was purified by silica gel column chromatography with hexane/ethyl acetate (3:1) as eluant to give **4c** (yellow oil) in 45% yield. − ^{1}H NMR (300 MHz, $CDCl_3$): δ = 0.89 (t, *J* = 7.3 Hz, 6 H, CH_3), 1.26 (m, 12 H, CH_2), 1.60 (m, 4 H, $COOCH_2CH_2$), 3.48 (s, 4 H, CH_2COO), 4.07 (t, *J* = 6.7 Hz, 4 H, $COOCH_2$), 7.20 (s, 2 H, H^α), 7.59 (m, 5 H, C_6H_5). − FT IR (film): $\tilde{\nu}$ = 1738 cm^{-1} (C=O ester), 1698 (C=O amide), 1170 (C−O). − MS (CI); *m*/*z* (%): 456 (100) [M$^+$].

Dioctyl *N*-Benzoylpyrrole-3,4-diacetate (4d): The crude product was purified by silica gel column chromatography with hexane/ethyl acetate (8:2) as eluant to give **4d** (yellow oil) in 41% yield. − ^{1}H NMR (300 MHz, $CDCl_3$): δ = 0.87 (t, *J* = 6.4 Hz, 6 H, CH_3), 1.26 (m, 20 H, CH_2), 1.62 (m, 4 H, $COOCH_2CH_2$), 3.49 (s, 4 H, CH_2COO), 4.08 (t, *J* = 6.8 Hz, 4 H, $COOCH_2$), 7.21 (s, 2 H, H^α), 7.48 (m, 2 H, H^m), 7.58 (t, *J* = 7.3 Hz, 1 H, H^p), 7.72 (d, *J* = 7.8 Hz, 2 H, H^o). − FT IR (film): $\tilde{\nu}$ = 1740 cm^{-1} (C=O ester), 1700 (C=O amide), 1170 (C−O). − MS (CI); *m*/*z* (%): 512 (100) [MH$^+$].

Didecyl *N*-Benzoylpyrrole-3,4-diacetate (4e): The crude product was purified by silica gel column chromatography with hexane/ethyl acetate (8:2) as eluant to give **4e** (yellow oil) in 43% yield. − ^{1}H NMR (100 MHz, $CDCl_3$): δ = 0.87 (t, *J* = 6.1 Hz, 6 H, CH_3), 1.25 (m, 28 H, CH_2), 1.61 (m, 4 H, $COOCH_2CH_2$), 3.48 (s, 4 H, CH_2COO), 4.07 (t, *J* = 6.9 Hz, 4 H, $COOCH_2$), 7.21 (s, 2 H, H^α), 7.59 (m, 5 H, C_6H_5). − FT IR (film): $\tilde{\nu}$ = 1738 cm^{-1} (C=O ester), 1700 (C=O amide), 1170 (C−O). − MS (CI); *m*/*z* (%): 569 (80) [MH$^+$].

Diundecyl *N*-Benzoylpyrrole-3,4-diacetate (4f): The crude product was purified by silica gel column chromatography with hexane/ethyl acetate (8:2) as eluant to give **4f** (yellow oil) in 42% yield. − ^{1}H NMR (100 MHz, $CDCl_3$): δ = 0.86 (t, *J* = 6.3 Hz, 6 H, CH_3), 1.24 (m, 32 H CH_2), 1.59 (m, 4 H, $COOCH_2CH_2$), 3.47 (s, 4 H, CH_2COO), 4.06 (t, *J* = 6.9 Hz, 4 H, $COOCH_2$), 7.20 (s, 2 H, H^α), 7.46 (m, 2 H, H^m), 7.56 (t, *J* = 7.2 Hz, 1 H, H^p), 7.71 (d, *J* = 7.7 Hz, 2 H, H^o). − FT IR (film): $\tilde{\nu}$ = 1743 cm^{-1} (C=O ester), 1700 (C=O amide), 1169 (C−O). − MS (CI); *m*/*z* (%): 596 (100) [M$^+$].

Didodecyl *N*-Benzoylpyrrole-3,4-diacetate (4g): The reaction time for this product was extended to 90 h. The crude product was purified by silica gel column chromatography with hexane/ethyl acetate (17:3) as eluant to give **4g** (yellow oil) in 38% yield. – ^{1}H NMR (300 MHz, $CDCl_3$): δ = 0.87 (t, *J* = 5.5 Hz, 6 H, CH_3), 1.25 (m, 36 H, CH_2), 1.61 (m, 4 H, $COOCH_2CH_2$), 3.48 (s, 4 H, CH_2COO), 4.07 (t, *J* = 6.9 Hz, 4 H, $COOCH_2$), 7.21 (s, 2 H, H^{α}), 7.45 (m, 2 H, H^{m}), 7.58 (t, *J* = 7.1 Hz, 1 H, H^{p}), 7.71 (d, *J* = 7.1 Hz, 2 H, H^{o}). – FT IR (film): $\tilde{\nu}$ = 1740 cm^{-1} (C=O ester), 1699 (C=O amide), 1166 (C–O). – MS (CI); *m*/*z* (%): 624 (100) [M^+].

Ditetradecyl *N*-Benzoylpyrrole-3,4-diacetate (4h): Due to the low solubility of tetradecyl alcohol in DMA, a mixture of DMA/ethyl ether (8:2) was used for this carbonylation. The reaction was carried at 60°C for 90 h. The crude prouct was purified by column chromatography on silica gel with hexane/ethyl acetate (8:2) as eluant to give **4h** (yellow oil) in 33% yield. – ^{1}H NMR (100 MHz, $CDCl_3$): δ = 0.86 (t, *J* = 5.9 Hz, 6 H, CH_3), 1.24 (m, 44 H, CH_2), 1.60 (m, 4 H, $COOCH_2CH_2$), 3.48 (s, 4 H, CH_2COO), 4.07 (t, *J* = 6.5 Hz, 4 H, $COOCH_2$), 7.21 (s, 2 H, H^{α}), 7.54 (m, 5 H, C_6H_5). – FT IR (film): $\tilde{\nu}$ = 1741 cm^{-1} (C=O ester), 1699 (C=O amide), 1179 (C–O). – MS (CI); *m*/*z* (%): 679 (100) [M^+].

General Procedure for the Hydrolysis of the *N*-Benzoylpyrrole-3,4-diacetates 3b–h: To a solution of dialkyl pyrrole-3,4-diacetate (2.93 mmol) in methanol (25 mL), kept under argon, triethylamine (14.06 mmol) was added. The solution was stirred for 14 h at room temperature. After removal of the solvent and triethylamine, the crude reaction mixture was purified by aluminum oxide column chromatography with hexane/ethyl acetate (3:1) as eluant.

Dipropyl Pyrrole-3,4-diacetate (3b): Yellow oil, yield 75%. – ^{1}H NMR (100 MHz, $CDCl_3$): δ = 0.91 (t, *J* = 7.3 Hz, 6 H, CH_3), 1.63 (m, 4 H, $COOCH_2CH_2$), 3.48 (s, 4 H, CH_2COO), 4.02 (t, *J* = 6.7 Hz, 4 H, $COOCH_2$), 6.61 (d, *J* = 2.5 Hz, 2 H, H^{α}), 8.41 (br. s, 1 H, NH). – FT IR (film): $\tilde{\nu}$ = 3395 cm^{-1} (NH), 1722 (C=O), 1172 (C–O). – MS (CI); *m*/*z* (%): 268 (100) [MH^+].

Dihexyl Pyrrole-3,4-diacetate (3c): Yellow oil, yield 60%. – ^{1}H NMR (100 MHz, $CDCl_3$): δ = 0.87 (t, *J* = 6.2 Hz, 6 H, CH_3), 1.26 (m, 12 H, CH_2), 1.54 (m, 4 H, $COOCH_2CH_2$), 3.48 (s, 4 H, CH_2COO), 4.05 (t, *J* = 6.6 Hz, 4 H, $COOCH_2$), 6.58 (d, *J* = 2.7 Hz, 2 H, H^{α}), 8.48 (br. s, 1 H, NH). – FT IR (film): $\tilde{\nu}$ = 3394 cm^{-1} (NH), 1734 (C=O), 1174 (C–O). – MS (CI); *m*/*z* (%): 352 (100) [M^+].

Dioctyl Pyrrole-3,4-diacetate (3d): Yellow oil, yield 74%. – ^{1}H NMR (100 MHz, $CDCl_3$): δ = 0.86 (t, *J* = 6.4 Hz, 6 H, CH_3), 1.27 (m, 20 H, CH_2), 1.60 (m, 4 H, $COOCH_2CH_2$), 3.50 (s, 4 H, CH_2COO), 4.06 (t, *J* = 6.8 Hz, 4 H, $COOCH_2$), 6.69 (d, *J* = 2.5 Hz, 2 H, H^{α}), 8.05 (br. s, 1 H, NH). – FT IR (film): $\tilde{\nu}$ = 3380 cm^{-1} (NH), 1740 (C=O), 1180 (C–O). – MS (CI); *m*/*z* (%): 408 (100) [MH^+].

Didecyl Pyrrole-3,4-diacetate (3e): Yellow oil, yield 75%. – ^{1}H NMR (100 MHz, $CDCl_3$): δ = 0.87 (t, *J* = 5.9 Hz, 6 H, CH_3), 1.25 (m, 28 H, CH_2), 1.60 (m, 4 H, $COOCH_2CH_2$), 3.49 (s, 4 H, CH_2COO), 4.05 (t, *J* = 6.6 Hz, 4 H, $COOCH_2$), 6.68 (d, *J* = 2.7 Hz, 2 H, H^{α}), 8.05 (br. s, 1 H, NH). – FT IR (film): $\tilde{\nu}$ = 3386 cm^{-1} (NH), 1738 (C=O), 1170 (C–O). – MS (CI); *m*/*z* (%): 463 (30) [M^+], 305 (100) [$M^+ - OC_{10}H_{21}$].

Diundecyl Pyrrole-3,4-diacetate (3f): Yellow oil, yield 66%. – ^{1}H NMR (100 MHz, $CDCl_3$): δ = 0.83 (t, *J* = 6.1 Hz, 6 H, CH_3), 1.21 (m, 32 H, CH_2), 1.55 (m, 4 H, $COOCH_2CH_2$), 3.43 (s, 4 H, CH_2COO), 4.00 (t, *J* = 6.6 Hz, 4 H, $COOCH_2$), 6.57 (d, *J* = 2.6 Hz, 2 H, H^{α}), 8.53 (br. s, 1 H, NH). – FT IR (film): $\tilde{\nu}$ = 3379 cm^{-1} (NH), 1734 (C=O), 1174 (C–O). – MS (CI); *m*/*z* (%): 492 (85) [MH^+], 319 (100) [$M^+ - HOC_{11}H_{23}$].

Didodecyl Pyrrole-3,4-diacetate (3g): White solid, mp 54°C, yield 75%. – ^{1}H NMR (100 MHz, $CDCl_3$): δ = 0.87 (t, *J* = 6.2 Hz, 6 H, CH_3), 1.25 (m, 36 H, CH_2), 1.61 (m, 4 H, $COOCH_2CH_2$), 3.49 (s, 4 H, CH_2COO), 4.06 (t, *J* = 6.5 Hz, 4 H, $COOCH_2$), 6.70 (d, *J* = 2.6 Hz, 2 H, H^{α}), 8.04 (br. s, 1 H, NH). – FT IR (film): $\tilde{\nu}$ = 3387 cm^{-1} (NH), 1734 (C=O), 1176 (C–O). – MS (CI); *m*/*z* (%): 521 (100) [MH^+].

Ditetradecyl Pyrrole-3,4-diacetate (3h): Due to the low solubility of **4g** in methanol, CH_2Cl_2 was added until the solution was homogeneous. A white solid (mp 63°C, yield 75%) was obtained as the product. – ^{1}H NMR (100 MHz, $CDCl_3$): δ = 0.87 (t, *J* = 6.1 Hz, 6 H, CH_3), 1.25 (m, 44 H, CH_2), 1.55 (m, 4 H, $COOCH_2CH_2$), 3.49 (s, 4 H, CH_2COO), 4.06 (t, *J* = 6.4 Hz, 4 H, $COOCH_2$), 6.71 (d, *J* = 2.6 Hz, 2 H, H^{α}), 8.04 (br. s, 1 H, NH). – FT IR (film): $\tilde{\nu}$ = 3379 cm^{-1} (NH), 1734 (C=O), 1175 (C–O). – MS (CI); *m*/*z* (%): 575 (80) [M^+], 361 (100) [$M^+ - COOC_{14}H_{29}$].

General Procedure for the Synthesis of the Octaalkyl Porphyrin-2,3,7,8,12,13,17,18-octaacetates H_2OAP: Paraformaldeyde (1.5 mmol) and dialkyl pyrrole-3,4-diacetate **3** (1.5 mmol) were added to 300 mL of dry CH_2Cl_2 in a 500-mL round-bottomed flask. The mixture was stirred under nitrogen for 15 min. $BF_3 \cdot Et_2O$ (0.15 mmol) was then added by syringe, and the reaction mixture was shielded from ambient light and stirred for 3.5 h. After this time, DDQ (0.68 mmol) and triethylamine (0.09 mmol) were added to oxidize the porphyrinogen and the reaction mixture was stirred for 20 h. A Vis spectrum of the crude reaction mixture showed a Soret band, indicative of porphyrin formation. Removal of the solvent under vacuum gave the crude product as red solid.

Octapropyl Porphyrin-2,3,7,8,12,13,17,18-octaacetate (H_2C_3OAP): The crude reaction mixture was purified by column chromatography on florisil with CH_2Cl_2/ethyl acetate (9:1) as eluant to give **H_2C_3OAP** (red solid) in 31% yield. – ^{1}H NMR (300 MHz, $CDCl_3$): δ = 0.82 (t, *J* = 7.4 Hz, 24 H, CH_3), 1.64 (m, 16 H, $COOCH_2CH_2$), 4.19 (t, *J* = 6.7 Hz, 16 H, $COOCH_2$), 5.20 (s, 16 H, CH_2COO), 10.32 (s, 4 H, H^{m}). – FT IR (film): $\tilde{\nu}$ = 1728 cm^{-1} (C=O), 1175 (C–O). – UV/Vis ($CHCl_3$): λ_{max} (log ε/$dm^3mol^{-1}cm^{-1}$ = 5.25) = 404 nm (Soret band), 501, 534, 573, and 627 (Q bands). – MS (CI); *m*/*z* (%): 1111 (100) [M^-]. – $C_{60}H_{78}N_4O_{16}$ (1111.3): calcd. C 64.85, H 7.07, N 5.04; found C 64.75, H 6.92, N 5.01.

Octahexyl Porphyrin-2,3,7,8,12,13,17,18-octaacetate (H_2C_6OAP): Crystallization from CH_2Cl_2/MeOH afforded **H_2C_6OAP** (red solid) in 67% yield. – ^{1}H NMR (300 MHz, $CDCl_3$): δ = 0.66 (t, *J* = 7.0 Hz, 24 H, CH_3), 1.11 (m, 48 H, CH_2), 1.62 (m, 16 H, $COOCH_2CH_2$), 4.21 (t, *J* = 7.0 Hz, 16 H, $COOCH_2$), 5.19 (s, 16 H, CH_2COO), 10.33 (s, 4 H, H^{m}). – FT IR (film): $\tilde{\nu}$ = 1727 cm^{-1} (C=O), 1168 (C–O). – UV/Vis ($CHCl_3$): λ_{max} (log ε/$dm^3mol^{-1}cm^{-1}$ = 5.24) = 406 nm (Soret band), 501, 534, 573, and 628 (Q bands). – MS (CI); *m*/*z* (%): 1447 (100) [$M^- - H$], 1448 (90) [M^-]. – $C_{84}H_{126}N_4O_{16}$ (1447.9): calcd. C 69.68, H 8.77, N 3.87; found C 69.52, H 8.58, N 3.98.

Octaoctyl Porphyrin-2,3,7,8,12,13,17,18-octaacetate (H_2C_8OAP): The crude reaction mixture was purified by column chromatography on florisil with CH_2Cl_2/ethyl acetate (19:1) as eluant to give **H_2C_8OAP** (red solid) in 37% yield. – ^{1}H NMR (300 MHz, $CDCl_3$): δ = 0.69 (t, *J* = 6.4 Hz, 24 H, CH_3), 1.16 (m, 80 H, CH_2), 1.59 (m, 16 H, $COOCH_2CH_2$), 4.18 (t, *J* = 6.7 Hz, 16 H, $COOCH_2$), 5.16 (s, 16 H, CH_2COO), 10.29 (s, 4 H, H^{m}). – FT IR (film): $\tilde{\nu}$ = 1730 cm^{-1} (C=O), 1180 (C–O). – UV/Vis ($CHCl_3$): λ_{max} (log ε/$dm^3mol^{-1}cm^{-1}$ = 5.22) = 406 nm (Soret band), 479,

523, 573, and 606 (Q bands). − MS (CI); *m/z* (%): 1672 (100) [M$^-$]. − $C_{100}H_{158}N_4O_{16}$ (1672.4): calcd. C 71.82, H 9.52, N 3.35; found C 72.06, H 9.77, N 3.11.

Octadecyl Porphyrin-2,3,7,8,12,13,17,18-octaacetate ($H_2C_{10}OAP$): The crude reaction mixture was purified by column chromatography on florisil with CH_2Cl_2/ethyl acetate (19:1) as eluant to give **$H_2C_{10}OAP$** (red solid) in 45% yield. − ^{1}H NMR (300 MHz, $CDCl_3$): δ = 0.74 (t, *J* = 7.2 Hz, 24 H, CH_3), 1.16 (m, 112 H, CH_2), 1.59 (m, 16 H, $COOCH_2CH_2$), 4.17 (t, *J* = 6.8 Hz, 16 H, $COOCH_2$), 5.15 (s, 16 H, CH_2COO), 10.29 (s, 4 H, H^m). − FT IR (film): $\tilde{\nu}$ = 1728 cm^{-1} (C=O), 1178 (C−O). − UV/Vis ($CHCl_3$): λ_{max} (log ε/dm^{3}mol^{-1}cm^{-1} = 5.21) = 406 nm (Soret band), 501, 534, 573, and 627 (Q bands). − MS (CI); *m/z* (%): 1896 (100) [M$^-$]. − $C_{116}H_{190}N_4O_{16}$ (1896.8): calcd. C 73.45, H 10.10, N 2.95; found C 73.49, H 10.01, N 3.01.

Octaundecyl Porphyrin-2,3,7,8,12,13,17,18-octaacetate ($H_2C_{11}OAP$): Crystallization from CH_2Cl_2/MeOH afforded **$H_2C_{11}OAP$** (red solid) in 68% yield. − ^{1}H NMR (300 MHz, $CDCl_3$): δ = 0.84 (t, *J* = 7.1 Hz, 24 H, CH_3), 1.13 (m, 128 H, CH_2), 1.60 (m, 16 H, $COOCH_2CH_2$), 4.20 (t, *J* = 6.9 Hz, 16 H, $COOCH_2$), 5.17 (s, 16 H, CH_2COO), 10.30 (s, 4 H, H^m). − FT IR (film): $\tilde{\nu}$ = 1725 cm^{-1} (C=O), 1183 (C−O). − UV/Vis ($CHCl_3$): λ_{max} (log ε/dm^{3}mol^{-1}cm^{-1} = 5.20) = 401 nm (Soret band), 502, 535, 573, and 628 (Q bands). − MS (CI); *m/z* (%): 2009 (100) [M$^-$]. − $C_{124}H_{206}N_4O_{16}$ (2009.0): calcd. C 74.13, H 10.33, N 2.79; found C 74.40, H 10.16, N 2.68.

Octadodecyl Porphyrin-2,3,7,8,12,13,17,18-octaacetate ($H_2C_{12}OAP$): The crude reaction mixture was purified by column chromatography on florisil with CH_2Cl_2/ethyl acetate (19:1) as eluant followed by crystallization from CH_2Cl_2/MeOH to give **$H_2C_{12}OAP$** (red solid) in 46% yield. − ^{1}H NMR (300 MHz, $CDCl_3$): δ = 0.83 (t, *J* = 7.0 Hz, 24 H, CH_3), 1.15 (m, 144 H, CH_2), 1.60 (m, 16 H, $COOCH_2CH_2$), 4.17 (t, *J* = 6.8 Hz, 16 H, $COOCH_2$), 5.15 (s, 16 H, CH_2COO), 10.28 (s, 4 H, H^m). − FT IR (film): $\tilde{\nu}$ = 1728 cm^{-1} (C=O), 1165 (C−O). − UV/Vis ($CHCl_3$): λ_{max} (log ε/dm^{3}mol^{-1}cm^{-1} = 5.17) = 406 nm (Soret band), 501, 534, 573, and 627 (Q bands). − MS (CI); *m/z* (%): 2121 (100) [M$^-$]. − $C_{132}H_{222}N_4O_{16}$ (2121.2): calcd. C 74.74, H 10.55, N 2.64; found C 75.08, H 10.76, N 2.31.

Octatetradecyl Porphyrin-2,3,7,8,12,13,17,18-octaacetate ($H_2C_{14}OAP$): The crude reaction mixture was purified by column chromatography on florisil with CH_2Cl_2/ethyl acetate (9:1) as eluant followed by crystallization from CH_2Cl_2/MeOH to give **$H_2C_{14}OAP$** (red solid) in 33% yield. − ^{1}H NMR (300 MHz, $CDCl_3$): δ = 0.85 (t, *J* = 7.0 Hz, 24 H, CH_3), 1.21 (m, 176 H, CH_2), 1.60 (m, 16 H, $COOCH_2CH_2$), 4.17 (t, *J* = 6.9 Hz, 16 H, $COOCH_2$), 5.15 (s, 16 H, CH_2COO), 10.28 (s, 4 H, H^m). − FT IR (film): $\tilde{\nu}$ = 1730 cm^{-1} (C=O), 1162 (C−O). − UV/Vis ($CHCl_3$): λ_{max} (log ε/dm^{3}mol^{-1}cm^{-1} = 5.15) = 406 nm (Soret band), 501, 534, 573, and 625 (Q bands). − MS (CI); *m/z* (%): 2346 (100) [M$^-$]. − $C_{148}H_{254}N_4O_{16}$ (2345.7): calcd. C 75.78, H 10.91, N 2.39; found C 75.40, H 10.55, N 2.11.

General Procedure for the Synthesis of the Octaalkyl 5,10,15,20-Tetraarylporphyrin-2,3,7,8,12,13,17,18-octaacetates (H_2OATPP): The aldehyde (1.00 mmol) and dialkyl pyrrole-3,4-diacetate **3** (1.00 mmol) were added to 100 mL of dry CH_2Cl_2 in a 250-mL round-bottomed flask. The mixture was stirred under nitrogen for 15 min. $BF_3 \cdot Et_2O$ (0.1 mmol) was added by syringe and the reaction mixture was shielded from ambient light and stirred for 1 h. After this time, DDQ (0.74 mmol) was added to oxidize the porphyrinogen and the reaction mixture was refluxed for 40 min. A Vis spectrum of the crude reaction mixture showed a Soret band, indicative of porphyrin formation. Removal of the solvent under vacuum gave the crude product as a green solid.

Octaoctyl 5,10,15,20-Tetraphenylporphyrin-2,3,7,8,12,13,17,18-octaacetate (H_2C_8OATPP): Purification by aluminum oxide column chromatography with CH_2Cl_2/MeOH (98:2) as eluant followed by flash aluminum oxide column chromatography with CH_2Cl_2 as eluant gave **H_2C_8OATPP** (green liquid paste) in 26% yield. − ^{1}H NMR (300 MHz, $CDCl_3$, 298 K): δ = 0.87 (t, *J* = 6.3 Hz, 24 H, CH_3), 1.26 (m, 80 H, CH_2), 1.40 (m, 16 H, $COOCH_2CH_2$), 3.16 (br. d, *J* = 17 Hz, 8 H, CH_2COO), 3.42 (br. d, *J* = 17 Hz, 8 H, CH_2COO), 3.76 (br. s, 16 H, $COOCH_2$), 7.71 (m, 12 H, H^{o,p}), 8.24 (m, 8 H, H^m). − ^{1}H NMR (300 MHz, $C_2D_2Cl_4$, 383 K): δ = 0.98 (t, *J* = 6.9 Hz, 24 H, CH_3), 1.34 (m, 96 H, CH_2), 3.25 (d, *J* = 17 Hz, 8 H, CH_2COO), 3.39 (d, *J* = 17 Hz, 8 H, CH_2COO), 3.77 (t, *J* = 6.9 Hz, 16 H, $COOCH_2$), 7.89 (m, 12 H, H^{o,p}), 8.50 (m, 8 H, H^m). − FT IR (film): $\tilde{\nu}$ = 1738 cm^{-1} (C=O), 1163 (C−O). − UV/Vis ($CHCl_3$): λ_{max} (log ε/dm^{3}mol^{-1}cm^{-1} = 5.16) = 458 nm (Soret band), 558, 606, and 714 (Q bands). − MS (CI); *m/z* (%): 1978 (100) [MH$^+$].

Octaoctyl 5,10,15,20-*p*-Octyloxytetraphenylporphyrin-2,3,7,8,12,13,17,18-octaacetate ($H_2C_8OAC_8TPP$): Purification by aluminum oxide column chromatography with CH_2Cl_2 as eluant [during the elution the polarity of the eluant was increased to CH_2Cl_2/MeOH (99:1)], followed by preparative TLC on aluminum oxide with CH_2Cl_2/MeOH (98:2), gave **$H_2C_8OAC_8TPP$** (green liquid) in 15% yield. − ^{1}H NMR (400 MHz, $CDCl_3$): δ = 0.86 (t, *J* = 7.1 Hz, 24 H, CH_3 β-chains), 0.95 (t, *J* = 7.6 Hz, 12 H, CH_3 $_m$-chains), 1.34 (m, 120 H, CH_2), 1.61 (m, 16 H, $COOCH_2CH_2$), 1.96 (m, 8 H, $C_6H_5OCH_2CH_2$), 3.19 (br. s, 8 H, CH_2COO), 3.42 (br. s, 8 H, CH_2COO), 3.76 (br. s, 16 H, $COOCH_2$), 4.17 (t, *J* = 6.5 Hz, 8 H, $C_6H_5OCH_2$), 7.19 (d, *J* = 8.1 Hz, 8 H, H^{3,5}), 8.24 (d, *J* = 8.1 Hz, 8 H, H^{2,6}). − FT IR (film): $\tilde{\nu}$ = 1740 cm^{-1} (C=O), 1603 and 1580 (C=C aryl), 1173 (C−O). − UV/Vis ($CHCl_3$): λ_{max} (log ε/dm^{3}mol^{-1}cm^{-1} = 5.13) = 463 nm (Soret band), 565, 614, and 723 (Q bands). − MS (CI); *m/z* (%): 2489 (100) [M$^-$].

Octadodecyl 5,10,15,20-*p*-Dodecyloxytetraphenylporphyrin-2,3,7,8,12,13,17,18-octaacetate ($H_2C_{12}OAC_{12}TPP$): Purification by aluminum oxide column chromatography with CH_2Cl_2 as eluant [during the elution the polarity of the eluant was increased to CH_2Cl_2/MeOH (99:1)], followed by preparative TLC on aluminum oxide with CH_2Cl_2/MeOH (98:2) gave **$H_2C_{12}OAC_{12}TPP$** (green liquid) in 23% yield. − ^{1}H NMR (300 MHz, $CDCl_3$): δ = 0.87 (m, 36 H, CH_3), 1.31 (m, 216 H, CH_2), 1.60 (m, 16 H, $COOCH_2CH_2$), 1.96 (m, 8 H, $C_6H_5OCH_2CH_2$), 3.20 (br. s, 8 H, CH_2COO), 3.41 (br. s, 8 H, CH_2COO), 3.72 (br. s, 16 H, $COOCH_2$), 4.18 (t, *J* = 6.6 Hz, 8 H, $C_6H_5OCH_2$), 7.21 (d, *J* = 7.8 Hz, 8 H, H^{3,5}), 8.11 (d, *J* = 7.8 Hz, 8 H, H^{2,6}). − FT IR (film): $\tilde{\nu}$ = 1740 cm^{-1} (C=O), 1603 and 1585 (C=C aryl), 1174 (C−O). − UV/Vis ($CHCl_3$): λ_{max} (log ε/dm^{3}mol^{-1}cm^{-1} = 5.13) = 462 nm (Soret band), 561, 615, and 723 (Q bands). − MS (CI); *m/z* (%): 3162 (80) [M$^-$], 3160 (100) [M$^-$ − 2 H].

General Procedure for the Synthesis of the Zinc Porphyrins ZnOAP: The free-base porphyrin (0.06 mmol) was dissolved in a saturated solution of $Zn(OAc)_2$ in 40 mL of dry DMF, containing NaOAc (0.30 mmol). The mixture was refluxed under nitrogen for 1 h. CH_2Cl_2 (40 mL) was added when the reaction vessel reached room temperature. The mixture was washed with brine (3 × 60 mL) and the metalated porphyrin was extracted with dichloromethane. The organic solution was dried with Na_2SO_4, filtered, and the solvent evaporated under reduced pressure.

(Octapropyl porphyrin-2,3,7,8,12,13,17,18-octaacetate)zinc (ZnC_3OAP): Crystallization from CH_2Cl_2/MeOH afforded the zinc por-

phyrin **ZnC$_3$OAP** (red solid) in 95% yield. − ^{1}H NMR (300 MHz, $CDCl_3$): δ = 0.80 (t, *J* = 7.4 Hz, 24 H, CH_3), 1.60 (m, 16 H, $COOCH_2CH_2$), 4.15 (t, *J* = 6.7 Hz, 16 H, $COOCH_2$), 5.18 (s, 16 H, CH_2COO), 10.31 (s, 4 H, H^m). − FT IR (film): $\tilde{\nu}$ = 1727 cm^{-1} (C=O), 1174 (C−O). − UV/Vis ($CHCl_3$): λ_{max} (log ε/dm^{3}mol^{-1}cm^{-1} = 5.44) = 406 nm (Soret band), 540 and 574 (Q bands). − MS (CI); *m*/*z* (%): 1174 (100) [M$^-$]. − $C_{60}H_{76}N_4O_{16}Zn$ (1174.7): calcd. C 61.35, H 6.52, N 4.77; found C 61.65, H 6.92, N 5.00.

(Octahexyl porphyrin-2,3,7,8,12,13,17,18-octaacetate)zinc (ZnC$_6$-OAP): Crystallization from CH_2Cl_2/MeOH afforded the zinc porphyrin **ZnC$_6$OAP** (red solid) in quantitative yield. − ^{1}H NMR (300 MHz, $CDCl_3$): δ = 0.66 (t, *J* = 7.1 Hz, 24 H, CH_3), 1.14 (m, 48 H, CH_2), 1.59 (m, 16 H, $COOCH_2CH_2$), 4.19 (t, *J* = 6.8 Hz, 16 H, $COOCH_2$), 5.12 (s, 16 H, CH_2COO), 10.16 (s, 4 H, H^m). − FT IR (film): $\tilde{\nu}$ = 1727 cm^{-1} (C=O), 1169 (C−O). − UV/Vis ($CHCl_3$): λ_{max} (log ε/dm^{3}mol^{-1}cm^{-1} = 5.41) = 405 nm (Soret band), 540 and 574 (Q bands). − MS (CI); *m*/*z* (%): 1512 (100) [M$^-$]. − $C_{84}H_{124}N_4O_{16}Zn$ (1511.3): calcd. C 66.76, H 8.27, N 3.71; found C 66.44, H 7.98, N 4.02.

(Octaoctyl porphyrin-2,3,7,8,12,13,17,18-octaacetate)zinc (ZnC$_8$-OAP): Crystallization from CH_2Cl_2/MeOH afforded the zinc porphyrin **ZnC$_8$OAP** (red solid) in 88% yield. − ^{1}H NMR (300 MHz, $CDCl_3$): δ = 0.71 (t, *J* = 7.0 Hz, 24 H, CH_3), 1.13 (m, 80 H, CH_2), 1.62 (m, 16 H, $COOCH_2CH_2$), 4.17 (t, *J* = 6.8 Hz, 16 H, $COOCH_2$), 5.17 (s, 16 H, CH_2COO), 10.29 (s, 4 H, H^m). − FT IR (film): $\tilde{\nu}$ = 1727 cm^{-1} (C=O), 1170 (C−O). − UV/Vis ($CHCl_3$): λ_{max} (log ε/dm^{3}mol^{-1}cm^{-1} = 5.40) = 404 nm (Soret band), 542 and 575 (Q bands). − MS (CI); *m*/*z* (%): 1735 (100) [M$^-$]. − $C_{100}H_{156}N_4O_{16}Zn$ (1735.7): calcd. C 69.20, H 9.06, N 3.23; found C 69.24, H 8.85, N 3.00.

(Octadecyl porphyrin-2,3,7,8,12,13,17,18-octaacetate)zinc (ZnC$_{10}$-OAP): Crystallization from CH_2Cl_2/MeOH afforded the zinc porphyrin **ZnC$_{10}$OAP** (red solid) in 97% yield. − ^{1}H NMR (300 MHz, $CDCl_3$): δ = 0.79 (t, *J* = 7.2 Hz, 24 H, CH_3), 1.12 (m, 112 H, CH_2), 1.63 (m, 16 H, $COOCH_2CH_2$), 4.19 (t, *J* = 6.9 Hz, 16 H, $COOCH_2$), 5.19 (s, 16 H, CH_2COO), 10.35 (s, 4 H, H^m). − FT IR (film): $\tilde{\nu}$ = 1729 cm^{-1} (C=O), 1179 (C−O). − UV/Vis ($CHCl_3$): λ_{max} (log ε/dm^{3}mol^{-1}cm^{-1} = 5.38) = 407 nm (Soret band), 542 and 575 (Q bands). − MS (CI); *m*/*z* (%): 1960 (100) [M$^-$]. − $C_{116}H_{188}N_4O_{16}Zn$ (1960.2): calcd. C 71.08, H 9.67, N 2.86; found C 71.40, H 9.61, N 3.03.

(Octaundecyl porphyrin-2,3,7,8,12,13,17,18-octaacetate)zinc (ZnC$_{11}$-OAP): Crystallization from CH_2Cl_2/MeOH afforded the zinc porphyrin **ZnC$_{11}$OAP** (red solid) in 73% yield. − ^{1}H NMR (300 MHz, $CDCl_3$): δ = 0.81 (t, *J* = 7.1 Hz, 24 H, CH_3), 1.17 (m, 128 H, CH_2), 1.63 (m, 16 H, $COOCH_2CH_2$), 4.18 (t, *J* = 6.9 Hz, 16 H, $COOCH_2$), 5.18 (s, 16 H, CH_2COO), 10.31 (s, 4 H, H^m). − FT IR (film): $\tilde{\nu}$ = 1721 cm^{-1} (C=O), 1166 (C−O). − UV/Vis ($CHCl_3$): λ_{max} (log ε/dm^{3}mol^{-1}cm^{-1} = 5.37) = 415 nm (Soret band), 543 and 576 (Q bands). − MS (CI); *m*/*z* (%): 2072 (100) [M$^-$]. − $C_{124}H_{204}N_4O_{16}Zn$ (2072.4): calcd. C 71.87, H 9.92, N 2.70; found C 72.08, H 10.03, N 2.59.

(Octadodecyl porphyrin-2,3,7,8,12,13,17,18-octaacetate)zinc (ZnC$_{12}$-OAP): Crystallization from CH_2Cl_2/MeOH afforded the zinc porphyrin **ZnC$_{12}$OAP** (red solid) in 98% yield. − ^{1}H NMR (400 MHz, $CDCl_3$): δ = 0.84 (t, *J* = 7.1 Hz, 24 H, CH_3), 1.16 (m, 144 H, CH_2), 1.62 (m, 16 H, $COOCH_2CH_2$), 4.17 (t, *J* = 6.9 Hz, 16 H, $COOCH_2$), 5.16 (s, 16 H, CH_2COO), 10.28 (s, 4 H, H^m). − FT IR (film): $\tilde{\nu}$ = 1722 cm^{-1} (C=O), 1170 (C−O). − UV/Vis ($CHCl_3$): λ_{max} (log ε/dm^{3}mol^{-1}cm^{-1} = 5.33) = 415 nm (Soret band), 544 and 576 (Q bands). − MS (CI); *m*/*z* (%): 2184 (100) [M$^-$]. − $C_{132}H_{220}N_4O_{16}Zn$ (2184.6): calcd. C 72.57, H 10.15, N 2.56; found C 72.66, H 9.93, N 2.47.

(Octatetradecyl porphyrin-2,3,7,8,12,13,17,18-octaacetate)zinc (ZnC$_{14}$-OAP): Crystallization from CH_2Cl_2/MeOH afforded the zinc porphyrin **ZnC$_{14}$OAP** (red solid) in quantitative yield. − ^{1}H NMR (400 MHz, $CDCl_3$): δ = 0.86 (t, *J* = 7.2 Hz, 24 H, CH_3), 1.19 (m, 176 H, CH_2), 1.64 (m, 16 H, $COOCH_2CH_2$), 4.19 (t, *J* = 7.2 Hz, 16 H, $COOCH_2$), 5.18 (s, 16 H, CH_2COO), 10.31 (s, 4 H, H^m). − FT IR (film): $\tilde{\nu}$ = 1729 cm^{-1} (C=O), 1172 (C−O). − UV/Vis ($CHCl_3$): λ_{max} (log ε/dm^{3}mol^{-1}cm^{-1} = 5.33) = 406 nm (Soret band), 542 and 575 (Q bands). − MS (CI); *m*/*z* (%): 2409 (100) [M$^-$]. − $C_{148}H_{252}N_4O_{16}Zn$ (2409.0): calcd. C 73.79, H 10.54, N 2.32; found C 74.02, H 10.67, N 2.37.

(Octaoctyl 5,10,15,20-tetraphenylporphyrin-2,3,7,8,12,13,17,18-octaacetate)zinc (ZnC$_8$OATPP): The crude reaction mixture was purified by preparative TLC on aluminum oxide with CH_2Cl_2 as eluant to give **ZnC$_8$OATPP** (green liquid) in 11% yield. − ^{1}H NMR (300 MHz, $CDCl_3$): δ = 0.86 (t, *J* = 6.9 Hz, 24 H, CH_3), 1.24 (m, 80 H, CH_2), 1.36 (m, 16 H, $COOCH_2CH_2$), 3.32 (br. s, 16 H, CH_2COO), 3.74 (t, *J* = 6.8 Hz, 16 H, $COOCH_2$), 7.66 (m, 12 H, $H^{o,p}$), 8.18 (m, 8 H, H^m). − FT IR (film): $\tilde{\nu}$ = 1734 cm^{-1} (C=O), 1170 (C−O). − UV/Vis ($CHCl_3$): λ_{max} (log ε/dm^{3}mol^{-1}cm^{-1} = 5.32) = 466 nm (Soret band), 603 and 662 (Q bands). − MS (CI); *m*/*z* (%): 2040 (100) [M$^-$]. − $C_{124}H_{172}N_4O_{16}Zn$ (2040.1): calcd. C 73.01, H 8.50, N 2.75; found C 72.81, H 8.29, N 2.84.

[Octaoctyl 5,10,15,20-tetrakis(*p*-octyloxyphenyl)porphyrin-2,3,7,8,12,13,17,18-octaacetate]zinc (ZnC$_8$OAC$_8$TPP): The crude reaction mixture was purified by silica gel column chromatography with CH_2Cl_2 as eluant to give **ZnC$_8$OAC$_8$TPP** (green liquid) in 21% yield. − ^{1}H NMR (300 MHz, $CDCl_3$, 300 K): δ = 0.85 (t, *J* = 7.1 Hz, 24 H, CH_3 β-chains), 0.94 (t, *J* = 7.0 Hz, 12 H, CH_3 *m*-chains), 1.33 (m, 120 H, CH_2), 1.61 (m, 16 H, $COOCH_2CH_2$), 1.96 (m, 8 H, $C_6H_5OCH_2CH_2$), 3.26 (br. s, 8 H, CH_2COO), 3.50 (br. s, 8 H, CH_2COO), 3.72 (br. s, 16 H, $COOCH_2$), 4.17 (t, *J* = 6.6 Hz, 8 H, $C_6H_5OCH_2$), 7.16 (d, *J* = 8.0 Hz, 8 H, $H^{3,5}$), 8.10 (d, *J* = 8.0 Hz, 8 H, $H^{2,6}$). − ^{1}H NMR (300 MHz, $CDCl_3$, 330 K): δ = 0.85 (t, *J* = 7.1 Hz, 24 H, CH_3 β-chains), 0.94 (t, *J* = 7.0 Hz, 12 H, CH_3 *m*-chains), 1.28 (m, 120 H, CH_2), 1.61 (m, 16 H, $COOCH_2CH_2$), 1.96 (m, 8 H, $C_6H_5OCH_2CH_2$), 3.42 (s, 16 H, CH_2COO), 3.75 (t, *J* = 6.9 Hz, 16 H, $COOCH_2$), 4.20 (t, *J* = 6.8 Hz, 8 H, $C_6H_5OCH_2$), 7.16 (d, *J* = 8.5 Hz, 8 H, $H^{3,5}$), 8.02 (d, *J* = 8.5 Hz, 8 H, $H^{2,6}$). − FT IR (film): $\tilde{\nu}$ = 1738 cm^{-1} (C=O), 1604 and 1580 (C=C aryl), 1170 (C−O). − UV/Vis ($CHCl_3$): λ_{max} (log ε/dm^{3}mol^{-1}cm^{-1} = 5.30) = 468 nm (Soret band), 609 and 669 (Q bands). − MS (CI); *m*/*z* (%): 2553 (100) [M$^-$]. − $C_{156}H_{236}N_4O_{20}Zn$ (2553.0): calcd. C 73.39, H 9.32, N 2.19; found C 73.10, H 9.62, N 1.97.

[Octadodecyl 5,10,15,20-tetrakis(*p*-dodecyloxyphenyl)porphyrin-2,3,7,8,12,13,17,18-octaacetate]zinc (ZnC$_{12}$OAC$_{12}$TPP): The crude reaction mixture was purified by silica gel column chromatography with CH_2Cl_2 as eluant to give **ZnC$_{12}$OAC$_{12}$TPP** (green liquid) in 32% yield. − ^{1}H NMR (300 MHz, $CDCl_3$, 300 K): δ = 0.88 (m, 36 H, CH_3), 1.31 (m, 216 H, CH_2), 1.60 (m, 16 H, $COOCH_2CH_2$), 1.95 (m, 8 H, $C_6H_5OCH_2CH_2$), 3.31 (br. s, 8 H, CH_2COO), 3.46 (br. s, 8 H, CH_2COO), 3.70 (br. s, 16 H, $COOCH_2$), 4.18 (t, *J* = 5.9 Hz, 8 H, $C_6H_5OCH_2$), 7.16 (d, *J* = 8.1 Hz, 8 H, $H^{3,5}$), 8.04 (d, *J* = 8.1 Hz, 8 H, $H^{2,6}$). − ^{1}H NMR (300 MHz, $CDCl_3$, 330 K): δ = 0.88 (m, 36 H, CH_3), 1.28 (m, 216 H, CH_2), 1.62 (m, 16 H, $COOCH_2CH_2$), 1.97 (m, 8 H, $C_6H_5OCH_2CH_2$), 3.42 (s, 16 H, CH_2COO), 3.75 (t, *J* = 6.9 Hz, 16 H, $COOCH_2$), 4.20 (t, *J* = 6.6 Hz, 8 H, $C_6H_5OCH_2$), 7.17 (d, *J* = 8.5 Hz, 8 H, $H^{3,5}$), 8.03 (d, *J* = 8.5 Hz, 8 H, $H^{2,6}$). − FT IR (film): $\tilde{\nu}$ = 1739 cm^{-1} (C=O),

1604 and 1585 (C=C aryl), 1172 (C−O). − UV/Vis ($CHCl_3$): λ_{max} (log ε/$dm^3mol^{-1}cm^{-1}$ = 5.22) = 468 nm (Soret band), 613 and 671 (Q bands). − MS (CI); *m/z* (%): 3226 (100) [M^-]. − $C_{204}H_{332}N_4O_{20}Zn$ (3226.3): calcd. C 75.95, H 10.37, N 1.74; found C 76.18, H 10.60, N 2.00.

(Octaoctyl 5,10,15,20-tetraphenylporphyrin-2,3,7,8,12,13,17,18-octaacetate)copper (CuC_8OATPP): The free-base porphyrin (0.02 mmol) was dissolved in a saturated solution of $Cu(OAc)_2$ in 40 mL of dry DMF containing NaOAc (0.24 mmol). The mixture was refluxed under nitrogen for 2 h. CH_2Cl_2 (40 mL) was added when the reaction vessel reached room temperature. The mixture was then washed with brine (3 × 60 mL) and the metalated porphyrin was extracted with dichloromethane. The organic solution was then dried with Na_2SO_4, filtered, and the solvent evaporated under reduced pressure. Purification by aluminum oxide column chromatography with CH_2Cl_2/hexane (9:1) as eluant gave **CuC_8OATPP** (green liquid paste) in 26% yield. − FT IR (film): $\tilde{\nu}$ = 1738 cm^{-1} (C=O), 1166 (C−O). − UV/Vis ($CHCl_3$): λ_{max} (log ε/$dm^3mol^{-1}cm^{-1}$ = 5.37) = 436 nm (Soret band), 574 (Q band). − MS (CI); *m/z* (%): 2038 (100) [M^-]. − $C_{124}H_{172}CuN_4O_{16}$ (2038.3): calcd. C 73.07, H 8.50, N 2.75; found C 73.45, H 8.78, N 3.01.

(Octadecyl porphyrin-2,3,7,8,12,13,17,18-octaacetate)palladium (PdC_{10}-OAP): The free-base porphyrin (0.06 mmol) was dissolved in a saturated solution of $Pd(OAc)_2$ in 40 mL of dry DMF containing NaOAc (0.30 mmol). The mixture was refluxed under nitrogen for 1 h. CH_2Cl_2 (40 mL) was added when the reaction vessel reached room temperature. The mixture was then washed with brine (3 × 60 mL) and the metalated porphyrin was extracted with dichloromethane. The organic solution was then dried with Na_2SO_4, filtered, and the solvent evaporated under reduced pressure. Crystallization from CH_2Cl_2/MeOH afforded the palladium porphyrin (red solid) in 88% yield. − ^{1}H NMR (300 MHz, $CDCl_3$): δ = 0.80 (t, *J* = 7.1 Hz, 24 H, CH_3), 1.16 (m, 112 H, CH_2), 1.63 (m, 16 H, $COOCH_2CH_2$), 4.19 (t, *J* = 7.0 Hz, 16 H, $COOCH_2$), 5.12 (s, 16 H, CH_2COO), 10.32 (s, 4 H, H^m). − FT IR (film): $\tilde{\nu}$ = 1727 cm^{-1} (C=O), 1170 (C−O). − UV/Vis ($CHCl_3$): λ_{max} (log ε/$dm^3mol^{-1}cm^{-1}$ = 5.37) = 402 nm (Soret band), 513 and 548 (Q bands). − MS (CI); *m/z* (%): 2001 (100) [M^-]. − $C_{116}H_{188}N_4O_{16}Pd$ (2001.2): calcd. C 69.62, H 9.47, N 2.80; found C 69.73, H 9.29, N 2.86.

(Octadecyl porphyrin-2,3,7,8,12,13,17,18-octaacetate)nickel (NiC_{10}-OAP): The free-base porphyrin (0.034 mmol) was dissolved in a solution of $Ni(OAc)_2$ (0.34 mmol) in 35 mL of glacial acetic acid. The mixture was refluxed under nitrogen for 1 h. CH_2Cl_2 (25 mL) was added when the reaction vessel reached room temperature. The mixture was then washed with brine (3 × 60 mL) and the metalated porphyrin was extracted with dichloromethane. The organic solution was then dried with Na_2SO_4, filtered, and the solvent evaporated under reduced pressure. Crystallization from CH_2Cl_2/MeOH afforded the nickel porphyrin (red solid) in 84% yield. − ^{1}H NMR (300 MHz, $CDCl_3$): δ = 0.80 (t, *J* = 7.1 Hz, 24 H, CH_3), 1.14 (m, 112 H, CH_2), 1.60 (m, 16 H, $COOCH_2CH_2$), 4.15 (t, *J* = 6.9 Hz, 16 H, $COOCH_2$), 4.99 (s, 16 H, CH_2COO), 10.00 (s, 4 H, H^m). − FT IR (film): $\tilde{\nu}$ = 1723 cm^{-1} (C=O), 1168 (C−O). − UV/Vis ($CHCl_3$): λ_{max} (log ε/$dm^3mol^{-1}cm^{-1}$ = 5.37) = 398 nm (Soret band), 521 and 555 (Q bands). − MS (CI); *m/z* (%): 1953 (100) [M^-]. − $C_{116}H_{188}N_4NiO_{16}$ (1953.5): calcd. C 71.32, H 9.70, N 2.87; found C 71.47, H 9.79, N 2.78.

(Octadecyl porphyrin-2,3,7,8,12,13,17,18-octaacetate)cadmium (CdC_{10}-OAP): The free-base porphyrin (0.06 mmol) was dissolved in a solution of $Cd(OAc)_2$ (0.6 mmol) in 50 mL of dry DMF containing NaOAc (0.23 mmol). The mixture was refluxed under nitrogen for 3 h. CH_2Cl_2 (25 mL) was added when the reaction vessel reached room temperature. The mixture was then washed with brine (3 × 60 mL) and the metalated porphyrin was extracted with dichloromethane. The organic solution was then dried with Na_2SO_4, filtered, and the solvent evaporated under reduced pressure. Crystallization from CH_2Cl_2/MeOH afforded the cadmium porphyrin (red solid) in 80% yield. − ^{1}H NMR (300 MHz, $CDCl_3$): δ = 0.81 (t, *J* = 7.1 Hz, 24 H, CH_3), 1.18 (m, 112 H, CH_2), 1.59 (m, 16 H, $COOCH_2CH_2$), 4.13 (t, *J* = 6.9 Hz, 16 H, $COOCH_2$), 4.94 (s, 16 H, CH_2COO), 9.74 (s, 4 H, H^m). − FT IR (film): $\tilde{\nu}$ = 1722 cm^{-1} (C=O), 1178 (C−O). − UV/Vis ($CHCl_3$): λ_{max} (log ε/$dm^3mol^{-1}cm^{-1}$ = 5.32) = 423 nm (Soret band), 553 and 588 (Q bands). − MS (CI); *m/z* (%): 2007 (100) [M^-]. − $C_{116}H_{188}CdN_4O_{16}$ (2007.2): calcd. C 69.41, H 9.44, N 2.79; found C 69.55, H 9.59, N 2.56.

(Octadecyl porphyrin-2,3,7,8,12,13,17,18-octaacetate)platinum (PtC_{10}-OAP): The free-base porphyrin (0.11 mmol) was dissolved in 40 mL of glacial acetic acid/toluene (7:3) containing NaOAc (0.61 mmol). The mixture was heated to 40°C and a solution of K_2PtCl_4 (0.23 mmol) in water (3.2 mL) was added. After that the mixture was heated to 90°C under nitrogen for 20 h. When the reaction vessel reached room temperature the mixture was filtered and dissolved in chloroform. Purification by silica gel column chromatography with CH_2Cl_2/AcOEt (39:19) as eluant gave the platinum porphyrin (pink solid) in 3% yield. − ^{1}H NMR (300 MHz, $CDCl_3$): δ = 0.79 (t, *J* = 7.2 Hz, 24 H, CH_3), 1.18 (m, 112 H, CH_2), 1.61 (m, 16 H, $COOCH_2CH_2$), 4.17 (t, *J* = 6.9 Hz, 16 H, $COOCH_2$), 5.06 (s, 16 H, CH_2COO), 10.23 (s, 4 H, H^m). − FT IR (film): $\tilde{\nu}$ = 1761 cm^{-1} (C=O), 1096 (C−O). − UV/Vis ($CHCl_3$): λ_{max} (log ε/$dm^3mol^{-1}cm^{-1}$ = 5.37) = 388 nm (Soret band), 507 and 538 (Q bands). − MS (CI); *m/z* (%): 2090 (100) [M^-]. − $C_{116}H_{188}N_4O_{16}Pt$ (2089.9): calcd. C 66.67, H 9.07, N 2.68; found C 66.71, H 9.09, N 2.50.

(Octadecyl porphyrin-2,3,7,8,12,13,17,18-octaacetate)lead (PbC_{10}-OAP): The free-base porphyrin (0.05 mmol) was dissolved in a solution of $Pb(OAc)_2$ (0.5 mmol) in dry THF (50 mL) and pyridine (3 mL). The mixture was refluxed under nitrogen for 16 h. CH_2Cl_2 (30 mL) was added when the reaction vessel reached room temperature. The mixture was then washed with brine (3 × 60 mL) and the metalated porphyrin was extracted with dichloromethane. The organic solution was then dried with Na_2SO_4, filtered, and the solvent evaporated under reduced pressure. Crystallization from CH_2Cl_2/MeOH afforded the lead porphyrin (green solid) in 90% yield. − ^{1}H NMR (300 MHz, $CDCl_3$): δ = 0.82 (t, *J* = 7.0 Hz, 24 H, CH_3), 1.13 (m, 112 H, CH_2), 1.61 (m, 16 H, $COOCH_2CH_2$), 4.16 (t, *J* = 6.8 Hz, 16 H, $COOCH_2$), 5.15 (dd, J_1 = 24.9, J_2 = 15.5, 16 H, CH_2COO), 10.34 (s, 4 H, H^m). − FT IR (film): $\tilde{\nu}$ = 1734 cm^{-1} (C=O), 1161 (C−O). − UV/Vis ($CHCl_3$): λ_{max} (log ε/$dm^3mol^{-1}cm^{-1}$ = 5.01) = 462 nm (Soret band), 586 (Q band). − MS (CI); *m/z* (%): 2102 (100) [M^-]. − $C_{116}H_{188}N_4O_{16}Pb$ (2102.0): calcd. C 66.28, H 9.01, N 2.66; found C 66.17, H 8.89, N 2.77.

(Octadecyl porphyrin-2,3,7,8,12,13,17,18-octaacetate)copper (Cu-C_{10}OAP): The free-base porphyrin (0.06 mmol) was dissolved in a solution of $Cu(OAc)_2$ (0.6 mmol) in 60 mL of glacial acetic acid. The mixture was refluxed under nitrogen for 1 h. CH_2Cl_2 (25 mL) was added when the reaction vessel reached room temperature. The mixture was then washed with brine (3 × 60 mL) and the metalated porphyrin was extracted with dichloromethane. The organic solution was then dried with Na_2SO_4, filtered, and the solvent evaporated under reduced pressure. Crystallization from CH_2Cl_2/MeOH afforded the copper porphyrin (red solid) in 63% yield. − FT IR (film): $\tilde{\nu}$ = 1727 cm^{-1} (C=O), 1170 (C−O). − UV/Vis ($CHCl_3$):

λ_{max} (log ε/dm^{3}mol^{-1}cm^{-1} = 5.37) = 404 nm (Soret band), 530 and 565 (Q bands). – MS (CI); *m/z* (%): 1958 (100) [M$^-$]. – $C_{116}H_{188}CuN_4O_{16}$ (1958.3): calcd. C 71.15, H 9.68, N 2.86; found C 71.27, H 9.69, N 3.00.

Acknowledgments

We thank Prof. G. Pelosi (University of Parma) and Prof. G. Gottarelli (University of Bologna) for helpful discussions. We acknowledge the Centro Interfacoltà di Misure of the University of Parma for instrumental facilities. This work was supported by MURST and CNR (Progetto Strategico and Progetto Tecnologie Chimiche Innovative).

[1] C. F. van Nostrum, R. J. M. Nolte, *J. Chem. Soc., Chem. Commun.* **1996**, 2385–2392.
[2] [2a] P. G. Schouten, J. M. Warman, M. P. de Haas, M. A. Fox, H.-L. Pan, *Nature* **1991**, *353*, 736–737. – [2b] C. Liu, H.-L. Pan, M. A. Fox, A. J. Bard, *Chem. Mater.* **1997**, *9*, 1422–1429.
[3] J. Simon, J.-J. André, *Molecular Semiconductors*, Springer-Verlag, Berlin, **1985**.
[4] For the first report of a mesogenic porphyrin see: J. W. Goodby, P. S. Robinson, B.-K. Teo, E. Cladi, *Mol. Cryst. Liq. Cryst., Lett. Sect.* **1980**, *56*, 303–309.
[5] [5a] E. Sartori, M. P. Fontana, M. Costa, E. Dalcanale, V. Paganuzzi, *Thin Solid Films* **1996**, *284–285*, 204–207. – [5b] E. Sartori, M. P. Fontana, E. Dalcanale, M. Costa, *Mol. Cryst. Liq. Cryst.* **1996**, *290*, 31–39.
[6] E. Dalcanale in *Comprehensive Supramolecular Chemistry*, vol. 10 (Eds.: J. L. Atwood, J. E. D. Davies, D. D. MacNicol, F. Vögtle, D. N. Reinhoudt), Pergamon, Oxford, **1996**, chapter 20.
[7] Y. Shimizu, M. Miya, A. Nagata, K. Ohta; I. Yamamoto, S. Kusabayashi, *Liq. Cryst.* **1993**, *14*, 795–805.
[8] [8a] Q. M. Wang, D. W. Bruce, *J. Chem. Soc., Chem. Commun.* **1996**, 2505–2506. – [8b] Q. M. Wang, D. W. Bruce, *Angew. Chem.* **1997**, *109*, 102–105; *Angew. Chem. Int. Ed. Engl.* **1997**, *36*, 150–152.
[9] [9a] L. R. Milgrom, G. Yahioglu, D. W. Bruce, S. Morrone, F. Z. Henari, W. J. Blau, *Adv. Mater.* **1997**, *9*, 313–315 – [9b] B. R. Patel, K. S. Suslick, *J. Am. Chem. Soc.* **1998**, *120*, 11802–11803.
[10] [10a] B. A. Gregg, M. A. Fox, A. J. Bard, *J. Chem. Soc., Chem. Commun.* **1987**, 1134–1135. – [10b] B. A. Gregg, M. A. Fox, A. J. Bard, *J. Am. Chem. Soc.* **1989**, *111*, 3024–3029.
[11] B. Frank, *Angew. Chem.* **1982**, *94*, 327–337; *Angew. Chem. Int. Ed. Engl.* **1982**, *21*, 343–353.
[12] A. Merz, R. Schropp, J. Lex, *Angew. Chem.* **1993**, *105*, 296–298; *Angew. Chem. Int. Ed. Engl.* **1993**, *32*, 291–293.
[13] J. S. Lindsey, I. C. Schreiman, H. C. Hsu, P. C. Kearney, A. M. Marguerettaz, *J. Org. Chem.* **1987**, *52*, 827–836.
[14] C. A. Hunter, J. K. M. Sanders, *J. Am. Chem. Soc.* **1990**, 112, 5525–5534.
[15] G. P. Chiusoli, M. Costa, S. Reverberi, *Synthesis* **1989**, 262–265.
[16] A. D. Adler, F. R. Longo, F. Kampas, J. Kim, *J. Inorg. Nucl. Chem.* **1970**, *32*, 2443–2445.
[17] G. D. Dorough, J. R. Miller, F. M. Huennekens, *J. Am. Chem. Soc.* **1951**, *73*, 4315–4320.
[18] D. W. Thomas, A. E. Martell, *J. Am. Chem. Soc.* **1959**, *81*, 5111–5119.
[19] W. R. Scheidt, in *The Porphyrins*, vol. 3 (Ed.: D. Dolphin), Academic Press, New York, **1979**, chapter 10.
[20] K. M. Barkigia, M. D. Berber, J. Fajer, C. J. Medforth, M. W. Renner, K. M. Smith, *J. Am. Chem. Soc.* **1990**, *112*, 8851–8857.
[21] For a related example with **SnOEP** see: J.-M. Barbe, C. Ratti, P. Richard, C. Lecomte, R. Gerardin, R. Guilard, *Inorg. Chem.* **1990**, *29*, 4126–4130.
[22] L. D. Sparks, C. J. Medforth, M.-S. Park, J. R. Chamberlain, M. R. Ondrias, M. O. Senge, K. M. Smith, J. A. Shelnutt, *J. Am. Chem. Soc.* **1993**, *115*, 581–592.
[23] C. J. Medforth, M. O. Senge, T. P. Forsyth, J. D. Hobbs, J. A. Shelnutt, K. M. Smith, *Inorg. Chem.* **1994**, *33*, 3865–3872.
[24] In the X-ray crystal structure of **CdTPP** the Cd^{II} ion is 0.578 Å out-of-plane of the N atoms: A. Hazell, *Acta Crystallogr.* **1986**, *C42*, 296–299.
[25] A. M. Levelut, *J. Chim. Phys.* **1983**, *80*, 149–161.
[26] J. Barberá, in *Metallomesogens – Synthesis, Properties and Applications* (Ed.: J. L. Serrano), VCH, Weinheim, **1996**, chapter 8.
[27] An out-of-plane displacement of the Pb^{II} ion of 1.17 Å has been estimated from the crystal structure of **PbTPrP**: K. M. Barkigia, J. Fajer, A. D. Adler; J. B. Williams, *Inorg. Chem.* **1980**, *19*, 2057–2061.
[28] By comparison the introduction of Pb^{II} in octasubstituted phthalocyanines does not lead to mesophase suppression, but to a large depression of both *K–D* and *D–I* transitions with respect to the corresponding free ligand. See: C. Piechocki, J.-C. Boulou, J. Simon, *Mol. Cryst. Liq. Cryst.* **1987**, *149*, 115–120 and references cited therein.
[29] D. M. Collard, C. P. Lillya, *J. Am. Chem. Soc.* **1991**, *113*, 8577–8583.
[30] W. R. Scheidt, Y. Lee, *Struct. Bonding* **1987**, *64*, 1–70.
[31] R. D. Shannon, *Acta Crystallogr.* **1976**, *A32*, 751–767.
[32] K. K. Anderson, J. D. Hobbs, L. Luo, K. D. Stanley, J. M. E. Quirke, J. A. Shelnutt, *J. Am. Chem. Soc.* **1993**, *115*, 12346–12352.
[33] J. E. Huheey, *Inorganic Chemistry*, 3rd ed., Harper International, Cambridge, **1983**.
[34] F. Lelj, G. Morelli, G. Riccardi, A. Roviello, A. Sirigu, *Liq. Cryst.* **1992**, *12*, 941–960.
[35] R. J. Abraham, F. Eivazi, H. Pearson, K. M. Smith, *J. Chem. Soc., Chem. Commun.* **1976**, 699–701.
[36] M. Costa, E. Dalcanale, G. Mori, unpublished results.

Received November 3, 1998
[O98493]